UNIVERSIDADE FEDERAL DE MINAS GERAIS
Escola de Engenharia
Programa de Pós-Graduação em Engenharia Metalúrgica, Materiais e de Minas

Manoel Vítor Borel Gonçalves

VALORIZAÇÃO SINÉRGICA DE VOLÁTEIS DE BIOMASSA E REJEITOS DE MINERAÇÃO DE FERRO

Belo Horizonte
2024

Manoel Vítor Borel Gonçalves

VALORIZAÇÃO SINÉRGICA DE VOLÁTEIS DE BIOMASSA E REJEITOS DE MINERAÇÃO DE FERRO

Tese apresentada ao Programa de Pós-Graduação em Engenharia Metalúrgica, Materiais e de Minas da Universidade Federal de Minas Gerais, como requisito parcial para a obtenção do título de Doutor em Engenharia Metalúrgica, Materiais e de Minas.

Orientador: Maurício Covcevich Bagatini

Coorientador: Ismael Vemdrame Flores

Belo Horizonte
2024

UNIVERSIDADE FEDERAL DE MINAS GERAIS
ESCOLA DE ENGENHARIA
Programa de Pós-Graduação em Engenharia
Metalúrgica, Materiais e de Minas

A tese intitulada **"Valorização Sinérgica de Voláteis de Biomassa e Rejeitos de Mineração de Ferro"**, área de concentração: Tecnologia Mineral, apresentada pelo candidato **Manoel Vítor Borel Gonçalves**, para obtenção do grau de Doutor em Engenharia Metalúrgica, Materiais e de Minas, foi aprovada pela comissão examinadora constituída pelos seguintes membros:

Documento assinado digitalmente
MAURICIO COVCEVICH BAGATINI
Data: 16/08/2024 07:05:42-0300
Verifique em https://validar.iti.gov.br

Dr. Maurício Covcevich Bagatini
Orientador (UFMG)

Documento assinado digitalmente
ISMAEL VEMDRAME FLORES
Data: 16/08/2024 07:20:09-0300
Verifique em https://validar.iti.gov.br

Dr. Ismael Vemdrame Flores
Coorientador (UFRJ)

Documento assinado digitalmente
JULIANA GONCALVES POHLMANN
Data: 19/08/2024 10:42:25-0300
Verifique em https://validar.iti.gov.br

Dra. Juliana Gonçalves Pohlmann
(Bionow)
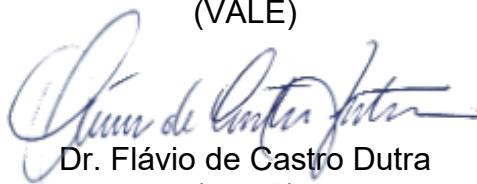
Documento assinado digitalmente
BRUNO DEVES FLORES
Data: 19/08/2024 15:41:19-0300
Verifique em https://validar.iti.gov.br

Dr. Bruno Deves Flores
(UFRGS)

Dr. Cláudio Batista Vieira
(UFOP)

Dr. Fabrício Vilela Parreira
(VALE)

Dr. Flávio de Castro Dutra
(VALE)

Documento assinado digitalmente
EDUARDO HENRIQUE MARTINS NUNES
Data: 03/12/2024 18:11:41-0300
Verifique em https://validar.iti.gov.br

_____
Coordenador do Programa de Pós-Graduação em
Engenharia Metalúrgica, Materiais e de Minas/UFMG

Belo Horizonte, 09 de agosto de 2024

Dedico esta Tese aos meus amados Pais, Marcos e Elaine Gonçalves, por todo amor, apoio e exemplos dedicados ao longo de toda minha vida. Dedico também a minha amada esposa, Daísa Gonçalves, pelo companheirismo e amor.

AGRADECIMENTOS

Agradeço primeiramente a Deus, pois sem Ele nada é possível, e por iluminar a minha caminhada, me dando força, determinação, foco e resiliência para superar todos os desafios presentes na construção da minha formação. Agradeço ao Nosso Senhor Jesus Cristo e a interseção da Virgem Maria por colocarem no meu caminho todas as pessoas que contribuíram com o desenvolvimento deste trabalho.

Agradeço profundamente aos meus amados Pais, Marcos e Elaine, por me proporcionarem muito mais que as condições necessárias para atingir esta formação. A minha trajetória não seria a mesma sem o constante apoio nas minhas escolhas e suporte proporcionado por eles. Por todo amor, confiança, ensinamentos e exemplos dedicados ao longo da minha vida, minha infinita gratidão!

Agradeço aos meus irmãos, Isabel e Luiz, por estarem sempre juntos a mim e pela compreensão nos momentos de dificuldade e ausência.

Agradeço a minha esposa Daísa, o amor da minha vida, minha companheira e amiga. Agradeço por todo apoio, carinho, amor e dedicação diária. Agradeço a compressão nos momentos de ausência e, principalmente, agradeço por estarmos juntos ao longo de toda a nossa formação profissional e por aceitar passar todos os seus dias ao meu lado. Externo também minha gratidão a toda a sua família.

Agradeço a toda a minha família, sem exceção.

Agradeço ao meu orientador Maurício Bagatini e ao meu coorientador Ismael Flores, em primeiro lugar pela oportunidade e confiança. Agradeço a parceria e amizade, a orientação e por todo o conhecimento compartilhado. Agradeço por todo apoio dedicado, pela paciência e pela oportunidade de aprender com eles.

Agradeço aos companheiros do Laboratório de Processo Siderúrgico da UFMG, por todas as experiências e conhecimentos compartilhados. Agradeço em especial, a Paula Maria e aos meus parceiros Lucas Mendonça e João Victor Rocha pelo auxílio na realização da parte experimental

RESUMO

A cadeia produtiva de ferro e aço é altamente dependente de combustíveis fósseis, fazendo com que o setor contribua com cerca de 8% de toda a emissão antropogênica de CO_2. Agentes redutores baseados em biomassa são considerados uma oportunidade para diminuir as emissões de CO_2 fóssil. Além dos gases de efeito estufa, grandes quantidades de resíduos sólidos também são geradas no setor mínero-metalúrgico, sendo o beneficiamento do minério de ferro responsável pela geração de cerca de 1,4 bilhões de toneladas de rejeitos por ano, o que torna latente e estratégica a sua recuperação em países com alta produção de minério de ferro. Nesse contexto, a presente Tese teve como propósito investigar a redução de óxidos de ferro a partir dos voláteis de biomassa, com foco na determinação dos fenômenos envolvidos e no impacto sinergético sobre os produtos sólidos e gasosos gerados. Na primeira etapa do trabalho, avaliou-se o potencial redutor da matéria volátil proveniente do eucalipto *in natura* e de finos de carvão vegetal sobre o minério de ferro granulado, visando compreender os fenômenos associados aos diferentes agentes redutores. Os resultados mostraram que até 980 °C ocorreu uma transformação mineralógica significativa, sendo a wüstita a fase majoritária obtida com ambos os tipos de biomassa. Testes interrompidos a 600 °C evidenciaram a deposição de carbono na superfície do minério, especialmente com eucalipto *in natura*. As características morfológicas da wüstita indicaram que o minério reduzido pelos voláteis da biomassa *in natura* teve o carbono depositado como principal agente redutor, enquanto a redução com voláteis do carvão vegetal se deu principalmente pelo H_2. A partir da primeira etapa, na qual se utilizou um minério de ferro de alto teor para reduzir a influência de impurezas e analisar com precisão os efeitos de agentes redutores de diferentes biomassas na mineralogia e morfologia do produto final, a segunda etapa expandiu a investigação. Ela explorou o efeito sinérgico dos voláteis do bagaço de cana-de-açúcar (SCB) em combinação com os óxidos de ferro presentes no rejeito de mineração de ferro (IOT), com foco na recuperação de ferro, na deposição de carbono no material ferroso e na produção de hidrogênio biogênico. Diferentes razões SCB/IOT foram testadas e observou-se que a menor quantidade de SCB em relação ao IOT proporcionou maior rendimento de H_2, resultante principalmente do craqueamento catalítico do alcatrão. Os ensaios a 1000 °C resultaram na obtenção de um material reduzido constituído de wüstita, faialita e ferro metálico, sendo que a maior proporção de biomassa favoreceu a metalização, atingindo 18,9% de Fe^0. Contudo, na temperatura de 600 °C foi possível obter um produto rico em magnetita (96,7%) e com 3,5% de C depositado, o que promoveu uma recuperação magnética de 98% em massa do total de rejeito tratado. Os resultados alcançados nesse trabalho propõem uma abordagem sinérgica tecnicamente viável para valorizar a matéria volátil resultante da pirólise de diferentes biomassas e como alternativa para a recuperação do ferro contido no montante de rejeitos de barragens da atividade minerária que atende a siderurgia.

Palavras-chave: voláteis de biomassa; craqueamento catalítico; deposição de carbono; hidrogênio biogênico; redução de óxidos de ferro; minério de ferro; rejeitos de mineração de ferro.

ABSTRACT

The iron and steel production chain is highly dependent on fossil fuels, causing the sector to contribute about 8% of all anthropogenic CO_2 emissions. Biomass-based reducing agents are considered an opportunity to reduce fossil CO_2 emissions. In addition to greenhouse gases, large amounts of solid waste are also generated in the mining and metallurgical sector, with iron ore beneficiation being responsible for generating approximately 1.4 billion tons of tailings per year, making their recovery crucial and strategic in countries with high iron ore production. In this context, the present Thesis aimed to investigate the reduction of iron oxides using biomass volatiles, focusing on determining the phenomena involved and the synergistic impact on the generated solid and gaseous products. In the first stage of the work, the reduction potential of volatiles from raw eucalyptus and charcoal fines on lump iron ore was evaluated, aiming to understand the phenomena associated with different reducing agents. The results showed that up to 980 ºC a significant mineralogical transformation occurred, with wüstite being the major phase obtained with both biomasses. Interrupted tests at 600 ºC evidenced carbon deposition on the ore surface, especially with raw eucalyptus. The morphological characteristics of wüstite indicated that the ore reduced by volatiles from raw biomass had carbon deposition as the main reducing agent, while the reduction with charcoal volatiles was mainly driven by H_2. Based on the first stage, in which high-grade iron ore was used to minimize the influence of impurities and accurately analyze the effects of reducing agents from different biomasses on the mineralogy and morphology of the final product, the second stage expanded the investigation. It explored the synergistic effect of volatiles from sugarcane bagasse (SCB) in combination with the iron oxides present in iron ore tailings (IOT), focusing on iron recovery, carbon deposition in the ferrous material, and the production of biogenic hydrogen. Different SCB/IOT ratios were tested, and it was observed that the lower SCB amount relative to IOT provided a higher H_2 yield, mainly resulting from tar catalytic cracking. The tests at 1000 ºC resulted in the production of a reduced material consisting of wüstite, fayalite, and metallic iron, with a higher biomass proportion favoring metallization, reaching 18.9% of Fe^0. However, at 600 ºC it was possible to obtain a product rich in magnetite (96.7%) with 3.5% deposited carbon, promoting a magnetic recovery of 98% by mass of the total treated tailings. The results achieved in this work propose a technically viable synergistic approach to valorize the volatile matter resulting from the pyrolysis of different biomasses and as an alternative for recovering iron contained in the amount of tailings from mining activities that supply the steel industry.

Keywords: biomass volatiles; catalytic cracking; carbon deposition; biogenic hydrogen; iron oxides reduction; iron ore; iron ore tailings.

LISTA DE FIGURAS

LISTA DE TABELAS

SUMÁRIO

1. INTRODUÇÃO, OBJETIVOS E ESTRUTURA DA TESE

1.1. Introdução

A produção do ferro e aço é um dos principais setores industriais e exerce grande influência na economia global e seu crescimento. Segundo a *World Steel Association* é previsto que até 2050 a utilização do aço aumente cerca de 1,2 vezes em comparação com os níveis atuais, visando a atender as demandas geradas pelo crescimento da população. No entanto, a indústria siderúrgica tradicionalmente emprega processos intensivos em energia, os quais são altamente dependentes de combustíveis fósseis (*e.g.*, carvão/coque e gás natural), principais responsáveis pelas emissões de gases de efeito estufa. Essa característica faz com que as emissões desse setor sejam próximas a 2,6 GtCO$_2$ por ano, correspondendo a 7-9% das emissões antropogênicas de CO$_2$ (Kim *et al*., 2022). Embora a indústria siderúrgica seja altamente dependente de energia fóssil, ela representa um dos pilares para o desenvolvimento da economia verde. Os setores e tecnologias que impulsionam a transição energética, como as fontes alternativas de energia, os veículos movidos a energia limpa, a infraestrutura eficiente na produção e transporte de combustível e as instalações de reciclagem, são todos dependentes dos produtos siderúrgicos.

Com os esforços crescentes de todos os setores industriais para alcançar emissões líquidas zero até 2050, é urgente e necessário desenvolver estratégias para descarbonizar a indústria siderúrgica. As estratégias de descarbonização têm se concentrado em medidas de eficiência energética, desenvolvimento de tecnologias disruptivas e substituição de fontes fósseis de energia e agentes redutores. Nesse sentido, a biomassa tem se mostrado como uma das fontes de energia mais promissoras e é particularmente atraente em regiões com alto potencial de desenvolvimento e com reservas limitadas de carvão metalúrgico de exploração economicamente viável, como o Brasil.

No entanto, o uso da biomassa *in natura* como fonte de energia na siderurgia enfrenta desafios técnicos consideráveis. A alta umidade e baixa densidade dificultam a logística, enquanto o baixo poder calorífico e o reduzido teor de carbono fixo limitam sua eficiência energética. Para aumentar sua densidade energética, diferentes tecnologias de conversão termoquímica, como a pirólise e a torrefação, são aplicadas. A matéria volátil constitui a grande parte da biomassa *in natura* (variando de 45-85% em massa, dependendo do teor de cinzas). Durante o tratamento térmico, essa matéria volátil é convertida em produtos não-condensáveis, como CO, CO$_2$, H$_2$ e

hidrocarbonetos leves (*e.g.*, CH$_4$), além de líquidos condensáveis, incluindo hidrocarbonetos pesados, como alcatrões e óleos.

Nos processos convencionais de produção de carvão vegetal, o aproveitamento da matéria volátil gerada ao longo do processamento termoquímico ainda é limitado, e grande parte desse material passa pela combustão em queimadores, sendo convertidos em CO$_2$, vapor d'água e calor. A emissão desses produtos representa um aumento na emissão de gases poluentes e um desperdício de uma rica fonte de gases e líquidos, o que também representa perdas econômicas do processo. Além disso, o Brasil se destaca por ter cerca de 23% da sua produção de ferro-gusa realizada com o uso do carvão vegetal. Devido à sua alta friabilidade, o material gera finos (moinha) durante a produção, manuseio e transporte, que são frequentemente usados como combustíveis adicionais injetados nos altos-fornos através de suas ventaneiras. No entanto, a alta reatividade da moinha limita sua aplicação em outros processos siderúrgicos como sinterização e coqueificação. Além disso, seu emprego na produção de aglomerados a frio, *e.g.* briquetes, é dificultado pela alta friabilidade e baixa densidade, entre outros fatores. Para superar essa limitação, é possível melhorar suas propriedades químicas por meio de tratamento termoquímico adicional, aproveitando a matéria volátil remanescente em processos alternativos.

O potencial redutor dos voláteis gerados durante o processamento termoquímico de biomassas foi mostrado por alguns autores (Strezov 2006; Guo *et al*., 2016; Bagatini *et al*., 2021; Yi *et al*., 2022). Além disso, o craqueamento catalítico da matéria volátil condensável promovida pela interação com minerais de ferro, enriquece os gases de pirólise em CO e H$_2$, além de promover a deposição de carbono sólido na superfície e nos poros do material ferroso, fornecendo condições adicionais para o progresso das reações de redução (Cahyono *et al*., 2014; Bagatini *et al*., 2021; Zulkania *et al*., 2021). Contudo, a capacidade desses materiais como fonte de agentes redutores, hidrogênio e carbono biogênicos precisam ser explorados para promover um melhor entendimento da viabilidade técnica.

Além dos gases de efeito estufa, a indústria do ferro e aço também produz quantidades substanciais de resíduos sólidos. A recorrente redução no teor dos minérios de ferro explorados atualmente faz com que etapas de beneficiamento se tornem indispensáveis, resultando em grandes quantidades de rejeitos, o que representa riscos ambientais consideráveis, como a contaminação do solo e da água. Anualmente, cerca de 1,4 bilhão de toneladas de rejeitos de

mineração de ferro (IOT) são geradas em todo o mundo. No Brasil, cerca de 270 milhões de toneladas desse tipo de rejeito são geradas e armazenadas em barragens (Levandoski *et al*., 2023). O teor de Fe nesses rejeitos geralmente varia entre 6% e 50% em peso, representando uma perda global entre 84 e 700 milhões de toneladas de Fe por ano. Em alguns casos, o teor de Fe total nos rejeitos pode ultrapassar 60%, o que agrava ainda mais essa perda. Portanto, a recuperação do metal contido nesses rejeitos é estratégica e fundamental para o desenvolvimento sustentável da indústria do ferro e aço. A literatura atual indica que os métodos mais comuns para a recuperação de Fe de IOT incluem separação física, flotação e magnetização via pré-redução (*i.e*., *magnetization roasting*). A pré-redução de rejeitos de mineração de ferro aumenta a diferença de magnetismo entre o mineral de ferro e a ganga, permitindo converter materiais fracamente magnéticos, como hematita e goethita, em magnetita que é fortemente magnética (Sahu *et al*., 2022).

Se de um lado a redução do consumo específico de energia associada às emissões de gases de efeito estufa está entre as principais prioridades da produção de ferro e aço, do outro, o manuseio e aproveitamento adequado dos rejeitos de barragem de minério de ferro são necessidades latentes da indústria minerária, diante dos custos e riscos associados as barragens em que tais resíduos são armazenados. Uma análise detalhada da sinergia entre a conversão termoquímica da biomassa e a redução dos óxidos de ferro para a recuperação de rejeitos é particularmente interessante para o cenário atual com foco na economia circular e no uso de fontes renováveis de carbono nos processos de produção de ferro. Para tanto, a investigação dos fenômenos que governam as reações decorrentes dos diferentes produtos formados em diferentes condições é essencial para elucidar a viabilidade técnica de possíveis rotas disruptivas que contribuam para aprimorar e transformar o panorama atual desses setores industriais.

1.1.1. Referências

Bagatini, M.C.; Kan, T.; Evans, T.J.; Strezov, V., 2021. Iron ore reduction by biomass volatiles. Journal of Sustainable Metallurgy. 7,215–226.

Cahyono, R.B.; Yasuda, N.; Nomura, T.; Akiyama, T., 2014. Optimum temperatures for carbon deposition during integrated coal pyrolysis–tar decomposition over low-grade iron ore for ironmaking applications. Fuel Processing Technology. 119,272–277.

Guo, D.; Zhu, L.; Guo, S.; Cui, B.; Luo, S.; Laghari, M.; Chen, Z.; Ma, C.; Zhou, Y.; Chen, J.; Xiao, B.; Hu, M.; Luo, S., 2016. Direct reduction of oxidized iron ore pellets using biomass syngas as the reducer. Fuel Processing Technology. 148,276-281.

Kim, J.; Sovacool, B.K.; Bazilian, M.; Griffiths, S.; Lee, J.; Yang, M.; Lee, J., 2022. Decarbonizing the iron and steel industry: A systematic review of sociotechnical systems, technological innovations, and policy options. Energy Research & Social Science. 89,102565.

Levandoski, W.M.K.; Ferrazo, S.T.; Bruschi, G.J.; Consoli, N.C.; Korf, E.P., 2023. Mechanical and microstructural properties of iron mining tailings stabilized with alkali-activated binder produced from agro-industrial wastes. Scientific Reports. 13,15754.

Sahu, S.N.; Meikap, B.C.; Biswal, S.K., 2022. Magnetization roasting of waste in ore beneficiation plant tailings using sawdust biomass; A novel approach to produce metallurgical grade pellets. Journal of Cleaner Production. 343,130894.

Strezov, V., 2006. Iron ore reduction using sawdust: Experimental analysis and kinetic modeling. Renewable Energy. 31,1892–1905.

Yi, L.; Zhang, N.; Hao, H.; Wang, L.; Xiao, H.; Li, G.; Liang, Z.; Huang, Z.; Jiang, T., 2022. Synergetic conversion laws of biomass and iron ore for syngas and direct reduced iron co-production. Journal of Cleaner Production. 363,132387.

Zulkania, A.; Rochmadi, R.; Cahyono, R.B.; Hidayat, M., 2021. Investigation into Biomass Tar-Based Carbon Deposits as Reduction Agents on Iron Ore Using the Tar Impregnation Method. Metals. 11,10,1623.

1.2. Objetivos

1.2.1. Objetivos gerais

A presente Tese foi realizada com o objetivo de investigar os fenômenos e os mecanismos envolvidos no processo de redução de óxidos de ferro por voláteis de biomassa por meio de testes simultâneos de pirólise e redução, visando a obtenção de condições favoráveis que promovam sinergicamente a redução de óxidos de ferro, a deposição de carbono e o aumento na geração de H_2 biogênico.

1.2.2. Objetivos específicos

Para atingir os objetivos gerais propostos, o presente estudo foi desenvolvido de acordo com os seguintes objetivos específicos:

- Conhecer a fenomenologia de redução dos óxidos de ferro por diferentes agentes voláteis da biomassa;

- Caracterizar morfologicamente os produtos de redução por voláteis;

- Verificar o efeito sinergético de redução, magnetização e deposição de carbono dos voláteis de bagaço de cana-de-açúcar sobre rejeito de mineração de ferro;

- Avaliar a geração de H_2 biogênico pelo efeito catalítico do rejeito de barragem sobre os voláteis oriundos da pirólise de bagaço de cana-de-açúcar;

- Determinar as condições que favorecem a ação combinada para agregar valor ao rejeito de minério de ferro e a biomassa.

1.3. Estrutura da Tese

A presente Tese foi organizada em sete capítulos. O Capítulo atual trata da introdução, dos objetivos e da estrutura da tese. Os capítulos 2 e 3 consistem em dois artigos publicados em periódicos internacionais.

O Capítulo 2 corresponde ao manuscrito do artigo publicado na edição especial "*New Approaches for Sustainable Steel Production and Processing*" do periódico internacional *Journal of Sustainable Metallurgy* (Qualis A2 – JIF 2,5) em junho de 2024. Nesta primeira etapa do estudo foram avaliados os perfis de vazão dos gases provenientes da pirólise do eucalipto *in natura* e do eucalipto carbonizado (carvão vegetal), com e sem a presença de minério de ferro. Após esta etapa, foram realizados ensaios interrompidos para avaliar qualitativamente, via microscopia eletrônica de varredura com microssonda EDS, o teor de carbono depositado na superfície do minério. Por fim, foram determinadas as participações majoritárias de cada agente redutor proveniente de cada uma das duas biomassas e qual o impacto na mineralogia e na morfologia dos produtos formados.

O Capítulo 3 corresponde ao manuscrito do artigo publicado no periódico internacional *Journal of Cleaner Production* (Qualis A1 – JIF 9,7) em novembro de 2024. Nesta etapa do estudo foram avaliadas 3 diferentes relações mássicas entre bagaço de cana-de-açúcar e rejeito de mineração de ferro, que foram aquecidas simultaneamente em quatro diferentes temperaturas. Estes ensaios foram realizados para avaliar quantitativamente quais as condições que favorecem a deposição de carbono, a produção de H_2 biogênico e a transformação mineralógica dos óxidos de ferro. Para isso, se utilizou análise de carbono, análise contínua de gases e difração de raios-X com refinamento Rietveld. Por fim, para cada condição testada foram determinados os percentuais de recuperação magnética a partir da massa total de rejeito tratado.

No Capítulo 4 serão apresentadas as considerações finais a respeito dos resultados obtidos e discutidos nos capítulos 2 e 3. Os principais resultados serão brevemente revisitados e analisados, destacando suas implicações e a contribuição para o campo de estudo.

O Capítulo 5 apresenta as contribuições originais para o conhecimento científico e o Capítulo 6 lista as publicações realizadas ao longo do período de desenvolvimento dessa Tese. Por fim,

o Capítulo 7 apresenta sugestões de trabalhos futuros que visam dar continuidade aos tópicos levantados ao longo desse estudo.

2. ARTIGO A. INVESTIGATION OF THE PHENOMENA ASSOCIATED WITH IRON ORE REDUCTION BY RAW BIOMASS AND CHARCOAL VOLATILES

Manoel V. B. Gonçalves[a*]; Lucas M. Mendonça[a]; Ismael V. Flores[b]; Maurício C. Bagatini[a]

[a] *Ironmaking Processes Laboratory (LPS), Department of Metallurgical and Materials Engineering, Federal University of Minas Gerais (UFMG), Av. Antônio Carlos, 6627, Bloco 2 – Sala 2242, Escola de Engenharia, 31.270-901, Belo Horizonte - MG, Brazil*

[b] *Federal University of Rio de Janeiro (UFRJ), Av. Horácio Macedo, 2030, Cidade Universitária, Centro de Tecnologia, Rio de Janeiro, 21.941-598, Brazil*

*Corresponding Author

Abstract

The volatile matter is the major constituent of the biomass but its potential as a reducing agent for iron oxides is still little explored, especially for carbonized biomass. In this study, the volatile products from raw biomass and charcoal were evaluated concerning their reducing potential of iron ore. Firstly, biomass samples were heated from room temperature up to 1000 ºC with a continuous outlet gas analysis. Following, these experiments were conducted under the same conditions with iron ore placed separately over the biomass bed. The heating of raw biomass and iron ore decreased the yield of CO and H_2, while CO_2 increased. When the charcoal was heated with iron ore, an increase in the yield of CO and CO_2 was observed, whereas the final volume of H_2 decreased. These results were associated with iron ore reduction by different agents and the tar catalytic cracking. From XRD, the magnetite was formed in all iron ore particle sizes and biomass, while wüstite was significantly identified only when the charcoal volatiles reacted with medium and fine ore. Interrupted tests carried out up to 600 ºC showed the ability of the biomass volatiles to pre-reduce the iron ore and deposit carbon on the surface of the ore from the tar catalytic cracking. From the experiments carried out up to 1000 ºC the morphology of wüstite indicated that hydrogen was the main reducing agent of the iron ore heated with charcoal, while deposited carbon was the reducing agent responsible for the ore morphology that was heated with raw biomass.

Keywords: Biomass volatiles; Iron ore reduction; Gas analysis; Catalytic cracking; Morphology

Graphical Abstract
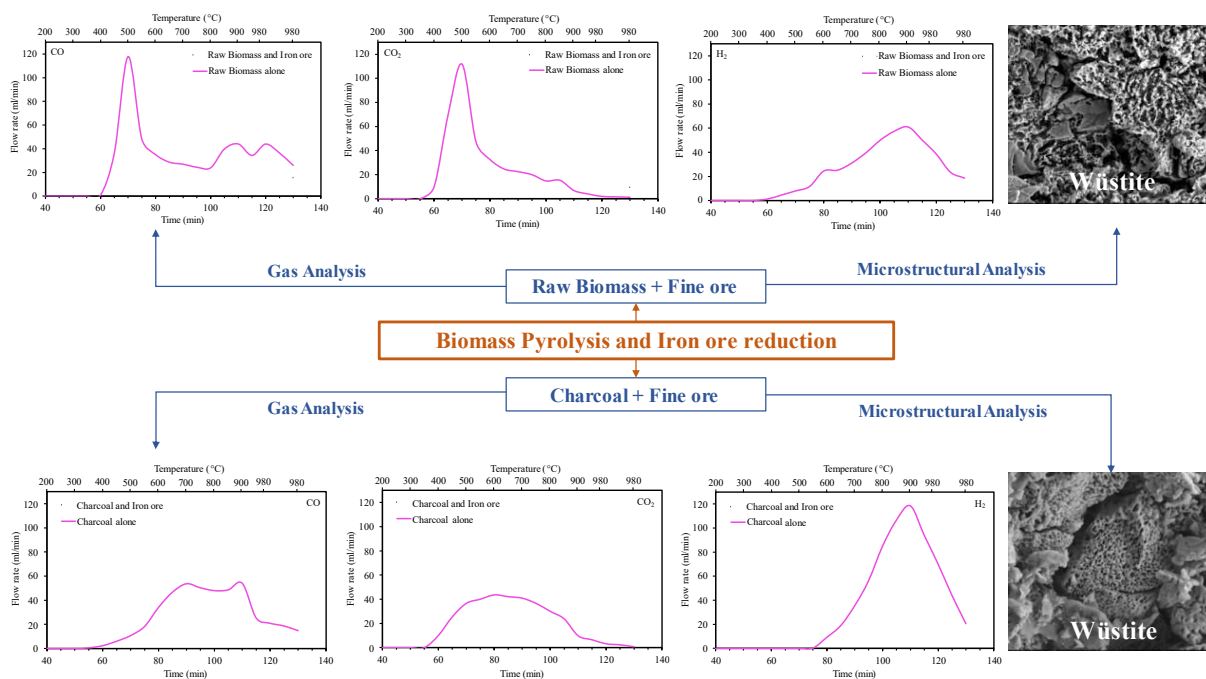
2.1. Introduction

Steel is the most used material by modern society since, besides its versatility in application and cost, it can be recycled without loss of properties. However, the iron and steelmaking industry is characterized by its energy-intensive processes, highly dependent on fossil fuels (*e.g.* coal and natural gas), which are the main ones responsible for greenhouse gas (GHG) emissions. According to the World Steel Association [1], in 2021 global crude steel production reached 1950.5 Mt, where, on average, each metric ton of steel released 1.85 metric tons of CO_2 into the atmosphere, which corresponded to approximately 8% of the total anthropogenic CO_2 emitted worldwide. Moreover, in the most common route of steel production (*i.e.*, blast furnace - basic oxygen furnace), the ironmaking step, including sintering, cokemaking, and blast furnace, accounts for about 90% of CO_2 emissions from an integrated steel plant [2].

Due to its high energy requirements and CO_2 emissions, strategies for the steel industry decarbonization have been strongly required, focusing on production efficiency improvement, which includes energy efficiency measures, production technologies innovation, and energy source/reducing agents switching [3]. Regarding the international scientific community, recent studies have showcased biomass as a highly promising energy source for the near-future decarbonization of the iron and steelmaking industry. Being worldwide distributed, biomass is a clean and sustainable resource, eco-friendly, with low cost, and considered carbon neutral [4-6]. This alternative is especially attractive for regions with limited reserves of coal and with a high potential for biomass development [7,8]. The low heating value and the low fixed carbon (C_{fix}) content are the main technical limitations to the use of raw biomass as an energy source. To increase its energy density, different pretreatment technologies like pyrolysis and torrefaction are applied to convert raw biomass into a solid product with suitable characteristics for the industry. The volatile matter is the main constituent of raw biomass (70-75% in mass [9,10]), which during thermal treatment is converted into non-condensable products, such as CO, CO_2, H_2, and light hydrocarbons (*e.g.*, CH_4) and condensable liquids (heavy hydrocarbons), such as tar and oils [11].

In ironmaking technologies, pre-reduction steps aim to improve energy efficiency and enable higher metallization during the main reduction stage. In the investigation of the feasibility of biomass syngas as a reducing for the direct reduction of iron ore pellets, Guo *et al*. [12] found that the biomass-derived syngas reduced the iron pellets with efficiency like that of natural gas,

converting the iron oxides in the pellets to metallic iron at 1173 K. Besides the non-condensable gases, iron ore can be reduced by tar. During direct reduction by biomass, organic molecules of tar compounds condense on the surface of iron ore particles and are cracked through reactions catalyzed by Fe, producing H_2, CO, CO_2, CH_4, other light hydrocarbons, and solid carbon [13]. The latter lay in direct contact with the iron ore surface (outer surface and pores) which ends up behaving like a self-reducing composite. Bagatini *et al*. [10], which investigated the iron ore reduction by biomass volatiles in a separate packed bed of biomass and iron ore, show that up to 800 ℃ iron ore reduction was governed by non-condensable gases, while above this temperature deposited solid carbon was the major reducing agent, making it possible the fully reduce iron ore at 1000 ℃. Moreover, Zulkania *et al*. [14] evaluated the optimum conditions for tar (recovered from waste biomass pyrolysis) impregnation and carbon deposition in porous iron ore. The authors have shown that carbon deposition was enhanced when the ratio of tar/iron ore was increased, and the formation of carbon deposits in iron ore improved the reduction rate of iron ore in tests up to 950 ℃. Biomass volatiles can also promote the recovery and recycling of minerals from industrial waste. For example, the generated waste iron ore beneficiation plant tailing can be a potential secondary iron resource for the ironmaking processes. Sahu *et al*. [15] evaluated the Fe recovery from the iron ore tailings by the magnetization roasting using sawdust biomass (SDB) as a reducing source. The study shows that at 950 ℃ and 15 min residence time, SDB could produce 65.34% Fe(T) of high-grade magnetite concentrate suitable for metallurgical-grade pellet production.

In Brazil, blast furnaces responsible for hot metal production are divided into coke blast furnaces, charcoal blast furnaces of integrated plants, and charcoal blast furnaces of independent producers who commercialize pig iron directly (non-integrated plant). In 2021, close to 23% of all Brazilian pig iron production was from charcoal-based production [16]. Brazil stands out for being the world's largest producer of charcoal. This product is a highly friable material, which undergoes high fragmentation from its production to its effective use in blast furnaces, resulting in 25-30% fine generation [17,18]. Charcoal fines with a particle size of less than 9 mm [19] are an alternative fuel with low added value without a consolidated use. Phenomena investigation of iron oxide reduction by biomass volatiles can elucidate the effective contribution of each reducing agent, which could offer advantages to understanding the best conditions for reduction using biomass, that will contribute to the path shortening of the use of these products in the steel industry. In this way, the purpose of this study was to

compare the reducing potential of the volatile matter released from raw biomass and charcoal fines, aiming to improve the volatiles use in the iron and steel industry.

2.2. Materials and Methods

2.2.1. Raw Materials

Eucalyptus (raw biomass) and charcoal (carbonized eucalyptus) from the Brazilian industry were used as sources of volatiles in the experiments. Both samples were employed with a particle size between 8.0 and 5.0 mm. The iron ore used was a lump hematite, which was crushed and sieved in three different particle size ranges: 8.0-6.3 mm (coarse), 5.6-3.36 mm (medium), and 2.3-0.84 mm (fine). The biomasses proximate analysis and the chemical composition of the iron ore are presented in Tables II.1 and II.2, respectively. The iron ore chemical composition was determined by X-ray fluorescence spectroscopy (XRF) and the loss on ignition (LOI) was measured from the mass loss of the samples through heating in a muffle furnace at 1000 ºC for 1 hour.

Table II.1. Proximate analysis of raw biomass and charcoal (weight %).

Components (db[a])	Raw biomass	Charcoal
Volatile matter	83.02	28.35
Fixed carbon	16.55	66.28
Ash	0.43	5.37

[a]dry basis

Table II.2. Chemical composition of iron ore (weight %).

Fe	O_{red}[a]	SiO_2	Al_2O_3	P_2O_5	CaO	K_2O	TiO_2	Mn	Cr	LOI[b]
67.95	29.20	0.75	0.50	0.024	0.05	0.01	0.03	0.14	0.02	0.32

[a]Reducible oxygen calculated from iron as hematite; [b]Loss on ignition.

2.2.2. Experimental Setup and Procedure

Two sets of experiments were carried out in the present study. The first one evaluated the chemical composition of pyrolysis gases released from the biomasses, while the second set aimed to investigate iron ore reduction by biomass volatiles. Figure 2.1a presents the schematic diagram of the experimental rig used in both test sets and a detailed description is found below.

These experiments were carried out in a vertical resistive furnace with a stainless steel reactor tube where the samples were heated in a graphite crucible. In the first set of tests (pyrolysis-only), 15 g of dried biomass (105 °C for 24 hours) were submitted to a constant N_2 flow of 1.5×10^3 Nml/min at a heating rate of 10 °C/min from room temperature up to 1000 °C, followed by a 15 min isotherm in this temperature. Throughout all the time of the experiments, the released gases were passed through a water condenser. After starting the experiments, all gases leaving the reactor traversed two condenser bottles, the first containing ice water and the second containing water at room temperature. This arrangement was assembled to ensure complete condensation of condensable products from biomasses pyrolysis. The secondary objective was to cool the gases and to safeguard the physical integrity of the gas analyzer. Following the condensation process, the gases traversed the piping system until reaching the ultimate purification stage, which involved passage through an activated carbon filter. This systematic arrangement guaranteed that the gases achieved room atmosphere conditions, which are required by the gas analyzer, facilitating gas precise characterization. The clean gas was continuously analyzed by the Online Infrared Syngas Analyzer (Gasboard 3100 – Cubic Ruiyi). The temperature in the sample was measured with a thermocouple. The average difference between the furnace and crucible thermal profiles for all experiments is shown in Figure 2.1b.

In the second set of experiments (pyrolysis-reduction tests) biomass and iron ore were simultaneously heated in separated beds (Figure 2.1c), where the pyrolytic gases flowed through the iron ore bed. Direct contact between the iron ore and the biomass was avoided. For that, 15 g of biomass and 15 g of iron ore were used, and all combinations of biomass (raw and charcoal) and iron ore particle size (coarse, medium, and fine) were evaluated. The same conditions of heating rate and atmosphere used in the pyrolysis-only experiments were employed and the resulting gas was continuously analyzed. After the 15 min isotherm, the furnace was turned off and the samples were naturally cooled using a N_2 atmosphere. At least three repetitions were carried out for each condition. From the repetitions carried out, the relative standard error for each gas measured was calculated to be approximately 4.9%.
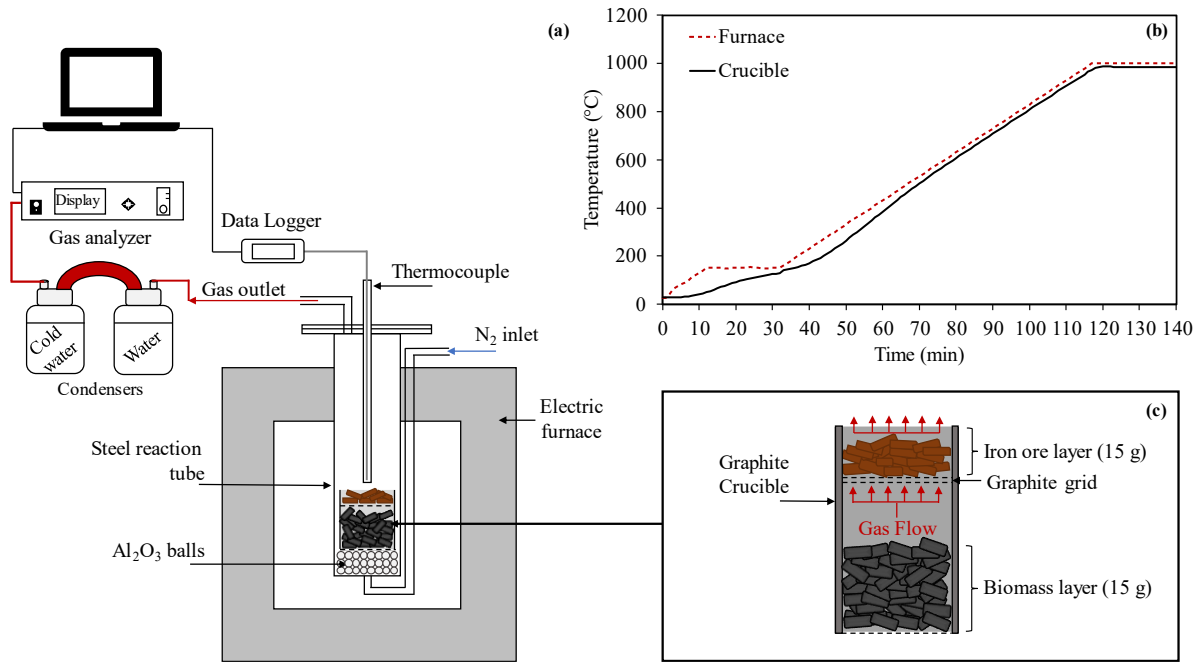
Figure 2.1. Schematic diagram of the experimental apparatus used for the pyrolysis and iron ore reduction tests.

After each experiment, the remaining material was collected and weighed. The iron ores reduction degree was calculated according to Equation 2.1, where m_0 is the initial mass of the iron ore sample, m_f is the sample mass of iron ore after the pyrolysis-reduction experiment, O_{red} is the mass of total reducible oxygen content in the iron ore (Table II.2) and M_{LOI} is the mass from iron ore loss on ignition (Table II.2).

$$RD\ (\%) = \left(\frac{(m_0 - m_f) - M_{LOI}}{O_{red}}\right) . 100 \tag{2.1}$$

In addition to the pyrolysis-reduction experiments described, interrupted tests were also carried out aiming to understand the participation of each reducing agent released from the biomass during the tests. The interrupted experiments employed the same conditions previously described (heating rate, isotherm, and cooling) but up to 600 ºC.

2.2.3. Phase Analysis and Microstructure

X-ray diffraction (XRD) analysis was used to identify the main mineral constituents contained in the iron ore before and after the experiments. For that, a Philips-PANalytical PW 1710

diffractometer was employed, using Cu (Kα) radiation at 2θ range from 3º to 90º, scan step size of 0.06º, the acquisition time of 3 s, tube voltage of 50 kV, and current of 35 mA. Phase identification was carried out using X'pert High Score Plus software. The Rietveld method, a refinement technique that uses XRD patterns to quantify the crystalline phases, was used to evaluate the mineralogical phases, using the same XRD software. The microstructure of these samples was also inspected by the field emission gun scanning electron microscope FEI Quanta FEG 3D microscope, consisting of a dual microscope with ion and electron beam, field effect emission electron gun, resolution of 0.8 nm for the electronic beam and 10 nm for the ion beam, focal length of 3 mm to 99 mm, and magnification of 24x to 800,000x in high and low vacuum. Backscattered electrons and energy dispersive X-ray spectroscopy (EDS) were used for the observation of microstructure and chemical analysis, respectively.

2.3. Results and Discussion

2.3.1. Pyrolytic Gases Analysis

First, the gaseous products from biomass pyrolysis alone were evaluated to understand the difference between the biomasses tested and to obtain a base scenario for further comparison with the experiments combining pyrolysis with iron ore. Figures 2.2a and b show the non-condensable gases flow rates during the pyrolysis of raw biomass and charcoal, respectively.

The main gaseous products identified for both samples were CH_4, CO, CO_2, and H_2. The gaseous products of the raw biomass were first detected around 350 ºC. The flow rate peaks of CO_2, CO, and CH_4 occurred simultaneously achieving maximum values close to 500 ºC, while H_2 reached a maximum near 900 ºC. For the charcoal, CO_2, CO, and CH_4 were also initially identified at around 350 ºC. Moreover, the flow rate peaks of these gases were shifted to the right, achieving maximum flow rate values at 600, 700, and 750 ºC, respectively. The H_2 was first detected just near 550 ºC with a maximum value at 900 ºC as well, the same as the raw biomass H_2 peak. It is worth mentioning that charcoal presented a more pronounced peak for H_2.

Close to 900 ºC raw biomass and charcoal presented an increase in CO flow rate, identified as a second peak, together with a drop in CH_4 and CO_2 flow rates. Such effect occurs because in

the last devolatilization stages, tar catalytic reforming [20] (2.2) and Boudouard reaction (2.3) might occur, with the latter being facilitated by the higher fixed carbon content of charcoal. That may be responsible for the increasing trends of CO and H_2 flow rates to the detriment of CH_4 and CO_2 in temperatures above 800 ºC [21-23]. Moreover, according to Strezov *et al.* [21], hydrogen is the most released gaseous product in the secondary thermal cracking of the evolved oils and reformation of the high-temperature vapor phase.

$$C_nH_{m(g)} + nCO_{2(g)} \rightarrow 2nCO_{(g)} + (\frac{m}{2})H_{2(g)} \tag{2.2}$$

$$C_{(s)} + CO_{2(g)} \leftrightarrow 2CO_{(g)} \tag{2.3}$$

Overall, the major differences between the raw eucalyptus and the charcoal are related to the previous thermal treatment that the charcoal was submitted during its production, which occurs at around 400 ºC. The original raw biomass was dried and partially devolatilized [21,24], decreasing the further release of CO, CO_2, and light hydrocarbons (*e.g.*, methane) from charcoal, as observed in Figure 2.2b. Thus, the more pronounced H_2 flow rate from charcoal must also be a consequence of this material being a more concentrated product toward gases that are released at higher temperatures [21].
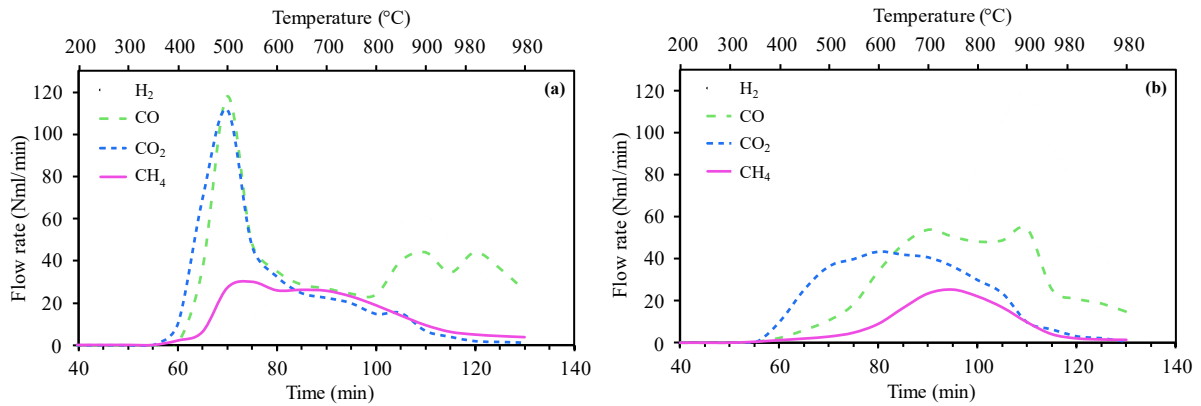
Figure 2.2. Pyrolysis gases from (a) raw biomass and (b) charcoal, in N_2 atmosphere at 10 ºC/min.

2.3.2. Pyrolytic Gas Analysis in the Presence of Iron Ore

The gas analysis resulting from the simultaneous heating of raw biomass or charcoal assembled with the iron ore layer (Figure 2.1) in three particle sizes is shown in Figures 2.3a and b. These

results were also compared with those from solely biomass or charcoal, presented in the previous section.

Like the biomasses alone, the flow rates for CH_4, CO, CO_2, and H_2 were initially identified close to 350 ℃. Although clear differences can be identified based on each biomass, the overall curves' profiles were the same but presented different magnitudes due to iron ore presence and the iron ore particle size. Regarding CO and CO_2, the contact of releasing gases with iron ore led to a drop in the CO flow rate with a consequent increase in the CO_2 flow rate throughout the experiment. This effect indicates that iron ore indirect reduction is occurring (2.4), consuming CO, and generating CO_2. In addition, the change in the magnitudes of the CO and CO_2 flow rate profiles were more significant for the finer iron ore.

$$Fe_xO_{y(s)} + CO_{(g)} \rightarrow Fe_xO_{y-1(s)} + CO_{2(g)} \tag{2.4}$$
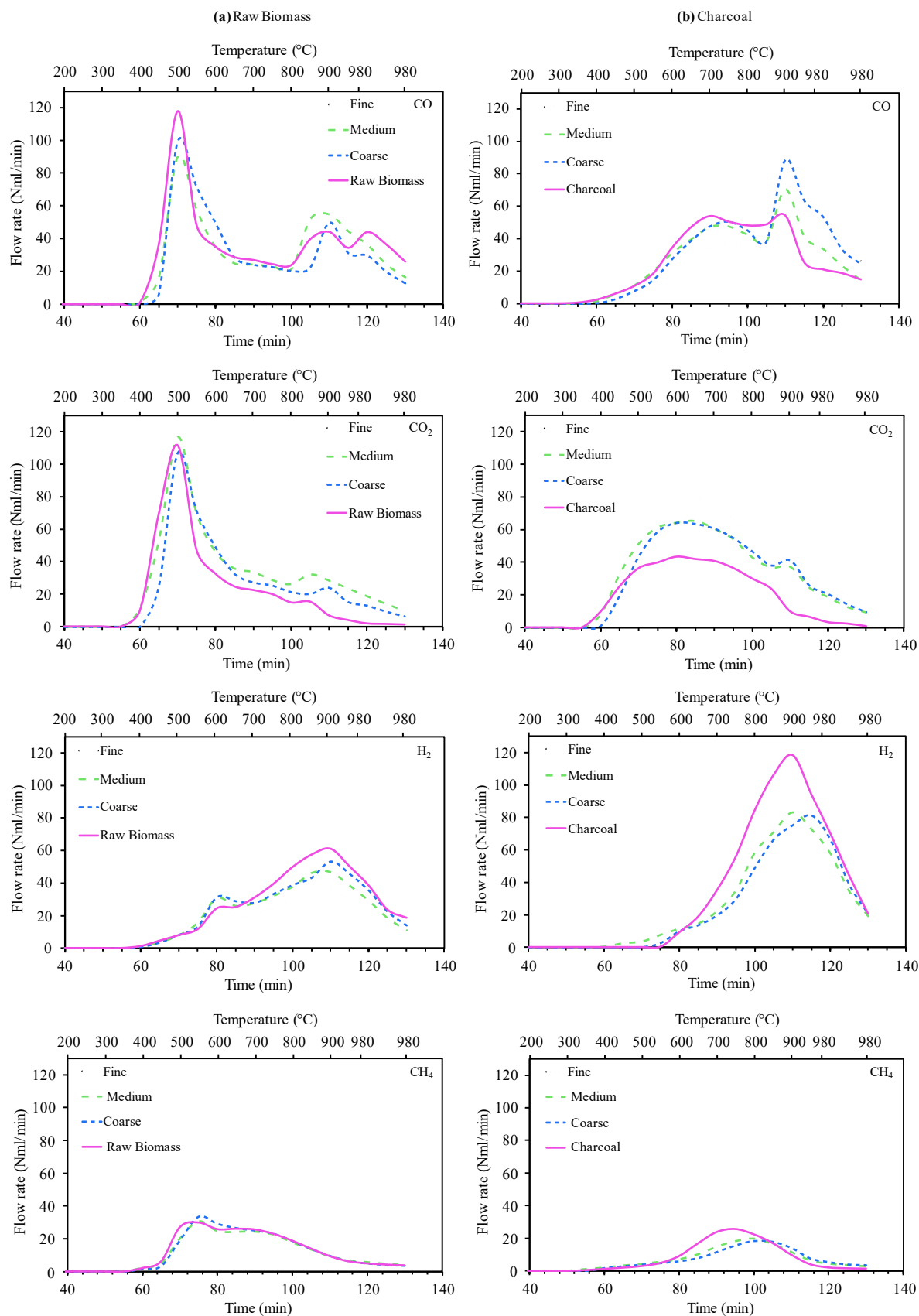
Figure 2.3. Gas analysis from (a) raw biomass and (b) charcoal during pyrolysis with iron ore in three different particle sizes.

For the H_2 flow rate profiles, differences due to iron ore particle size were more pronounced when using raw biomass, with the finer ores achieving smaller H_2 profiles. Such differences were relatively small when using charcoal, especially above 600 ºC. The higher H_2 flow rate seen in the range of 500-600 ºC for raw biomass and up to 600 ºC for charcoal, compared to the baseline, indicates the occurrence of secondary reactions, such as tar cracking. According to Hata *et al*. [25] and Li *et al*. [26], tar is significantly released in the primary devolatilization of biomass from the pyrolysis/depolymerization/breaking down of the biomass components (cellulose, hemicellulose, and lignin) between 400 and 600 ºC. It is known that temperatures above 1100 ºC are required for efficient tar cracking [27], however, it is well established that iron oxides can be an effective catalyst for tar conversion. In the presence of iron ore, above 500 ºC the primary tar condenses on the particles' surface, which is catalytically cracked and reformed into solid carbon, smaller light non-condensable gases (*e.g*., CO and H_2), and hydrocarbons with lower molar mass [13].

Further, the lowest H_2 flow rate for both biomasses above 600 ºC is probably related to the consumption of this gas through the global reduction reaction shown in (2.5). According to Oh & Noh [28], at high temperatures, H_2 can exert a more notable reduction effect than CO due to diffusional issues and its endothermic character of reducing reaction.

$$Fe_xO_{y(s)} + H_{2(g)} \rightarrow xFe_{(s)} + yH_2O_{(g)} \tag{2.5}$$

For the temperature ranges of 800-900 ºC for raw biomass, and 850-900 ºC for charcoal, it can be seen in Figures 2.3a and b that CO and CO_2 increase forming a secondary peak. It may indicate the occurrence of coupled reactions of deposited solid carbon gasification (2.6) and iron ore reduction (2.7). Although CO reacts with iron oxides, the CO flow rate is more noticeable than that of CO_2. It reveals that the carbon gasification rate is possibly greater than the reduction rate by CO, especially at higher temperatures. Moreover, although the rate of the solid-state iron ore reduction through reactions like those shown in (2.8) is much slower than the gaseous reduction reaction, that reaction can also contribute to the simultaneous peak of CO and CO_2 [29].

$$C_{(s)} + CO_{2(g)} \leftrightarrow 2CO_{(g)} \tag{2.6}$$

$$Fe_xO_{y(s)} + CO_{(g)} \rightarrow xFe_{(s)} + CO_{2(g)} \tag{2.7}$$

$$Fe_xO_{y(s)} + C_{(s)} \rightarrow Fe_xO_{y-1(s)} + CO_{(g)} + CO_{2(g)} \tag{2.8}$$

Through gas analysis shown in Figure 2.3, it was possible to identify a very small variation in methane flow rate profiles, for each of the biomasses. Direct reduction of the iron oxide with methane is too complex to occur in a single step [30]. For methane to participate in reduction reactions, the molecule needs to be cracked into C(s) and H_2(g). According to Lee [31], this process occurs above 1000 ℃, a temperature which was not reached in the experiments carried out. Furthermore, the reduction kinetics by primarily released volatiles is superior to the reduction by methane [30], that being a reducing agent of secondary importance when compared to CO and H_2. The latter justifies the small variations in the CH_4 flow rate profiles seen in Figure 2.3.

The total gas yields during the raw biomass and charcoal pyrolysis, with or without iron ore in three different particle sizes are shown in Figures 2.4a and b, respectively. According to Figure 2.4, a slight variation is observed in the overall volume of non-condensable gases released from the two biomasses. For raw biomass, the total volume of gases generated amounted to 8.09×10^3 Nml, whereas for charcoal the total volume reached 8.14×10^3 Nml. Raw biomass has around three times more volatile matter than charcoal when considered on a mass basis. However, when considering the volume of gases, it is necessary to consider the biomass constituents and their degradation temperatures. As shown in Figures 2.2 and 2.4, the main gases released in the pyrolysis of raw biomass, which contribute significantly to the total volume of non-condensable volatile matter, are CO and CO_2. The release profile of CO and CO_2 differs considerably between the two biomasses. For raw biomass, the flow rate of CO and CO_2 is significantly higher because in charcoal these gases are released significantly at the production temperature, which occurs close to 400 ℃, due to the greater degradation of cellulose and hemicellulose. For CH_4, the variation in the release profile is slightly relevant because cellulose, hemicellulose, and lignin contribute to the release of CH_4 at low, medium, and high temperatures [32]. After the charcoal production process, the primary fractions of hemicellulose and cellulose undergo degradation, leaving the charcoal enriched in lignin and its derived compounds. The similarity in the volumes of gases released by the two biomasses can be attributed to the substantial release of hydrogen during the additional carbonization of charcoal. Moreover, the mass of lignin and its derivatives, which can be converted into hydrogen, is significantly greater in charcoal compared to raw biomass. As a result, even though the theoretically lower content of non-condensable volatiles in charcoal, this discrepancy is volumetrically compensated by the increased presence of hydrogen stemming from the abundant availability of lignin and its derivatives. Moreover, as mentioned in the previous section, some gasification reactions in the

biomass bed may occur, especially for beds richer in solid C, such as charcoal. These reactions, such as the Boudouard reaction, can contribute to promoting an increase in the volume of gases generated concerning the gases intrinsically contained in the biomasses.

For simultaneous heating of raw biomass and iron ore, the yield of reducing gases (CO and H_2) was lower than that for biomass only, while the volume of CO_2 increased. Regarding the latter, the same behavior was observed for charcoal, however, the total volume of CO also increased. In the case of charcoal, it is possible that carbon gasification and solid-state reduction occurred in greater magnitude than the iron oxide gaseous reduction, generating CO overall. That can also be seen by the large increase in the second CO peaks in Figure 2.3b, more pronounced than the raw biomass (Figure 2.3a). Furthermore, it is important to note that the simultaneous occurrence of the second flow rate peak of CO and the flow rate peak of H_2, close to 900 ºC, can induce a majority reduction by hydrogen.
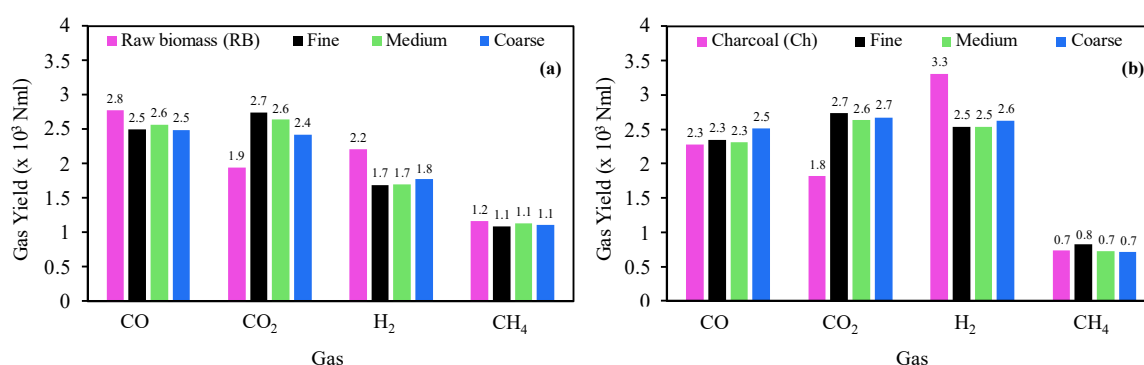
Figure 2.4. Gaseous products yield for (a) raw biomass and (b) charcoal pyrolysis at 980 ºC with and without iron ore in three different particle sizes.

2.3.3. X-ray Diffraction Analysis

Figures 2.5a and b give the phases identified by X-ray diffraction (XRD) in iron ore before and after heating with the two biomasses. The Rietveld analysis results of these XRD patterns are shown in Figure 2.5c.
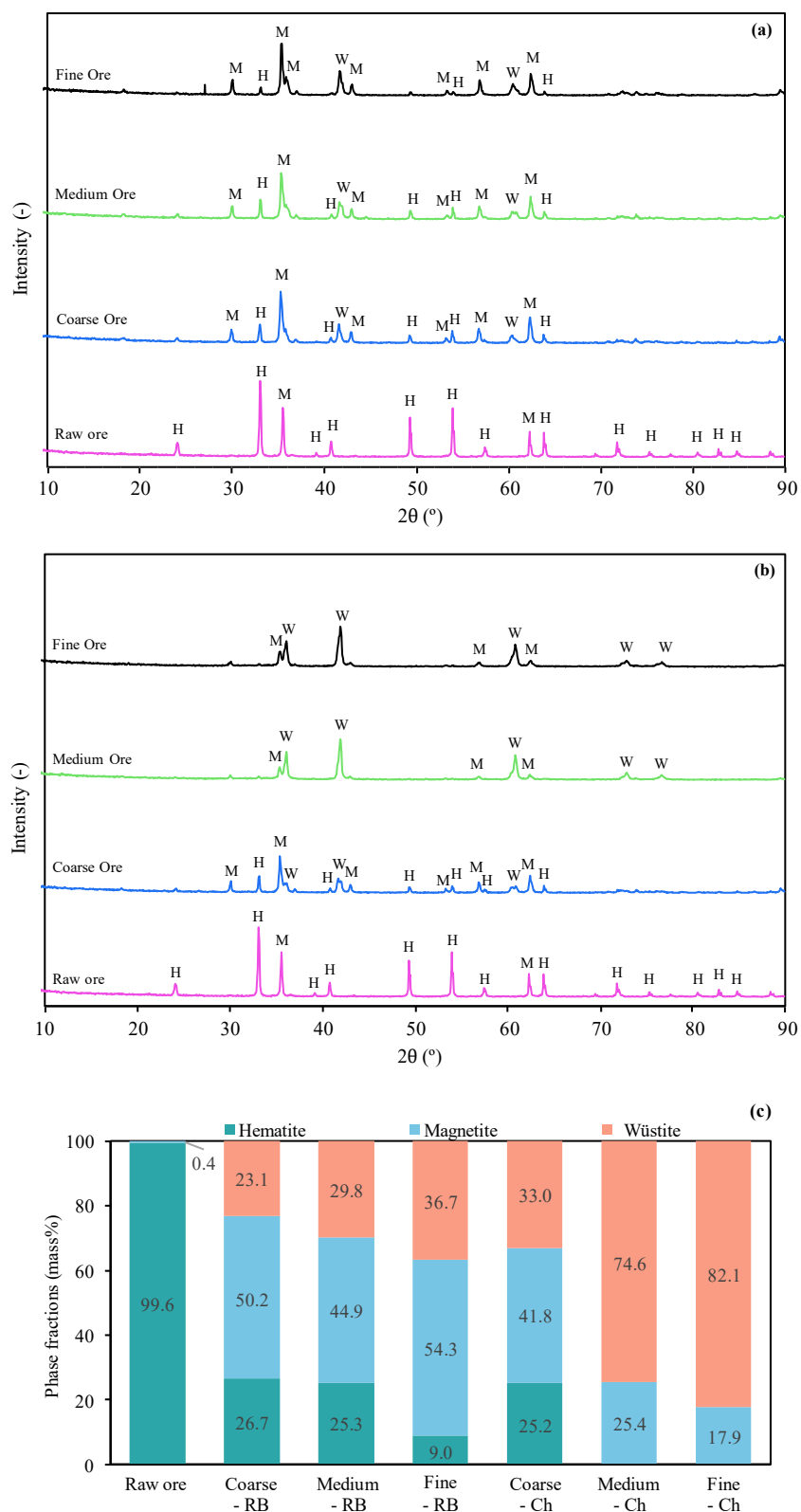
Figure 2.5. XRD patterns of raw iron ore and iron ore at different particle sizes heated with (a) raw biomass and (b) charcoal, at 980 °C, where H: hematite; M: magnetite; W: wüstite; (c) phase fractions determined by the Rietveld analysis, where RB: raw biomass; Ch: charcoal.

Figure 2.5 shows hematite as the major mineral in the raw iron ore used. According to Figures 2.5a and c, for all ore particle sizes heated with raw biomass, the major crystalline species identified was magnetite. This indicates that the first reduction step (hematite → magnetite) was the dominant reaction, and the second reduction step (magnetite → wüstite) occurred moderately. On the other hand, hematite completely disappeared and wüstite was the dominating phase for fine and medium samples heated with charcoal (Figure 2.5b and c), which indicates a remarkable advance in iron oxides reduction. For the coarse ore, heated with charcoal, although there was slightly greater wüstite formation than when ore of this particle size reacted with raw biomass, magnetite remained as the majority phase, which indicates little progress in iron oxide reduction.

2.3.4. Reduction Degree

The iron ore mass losses obtained from the reduction tests allowed the reduction degree (RD) for the three iron ore particle sizes to be calculated. The reduction degree (calculated according to Equation 1.1) is presented in Figure 2.6.
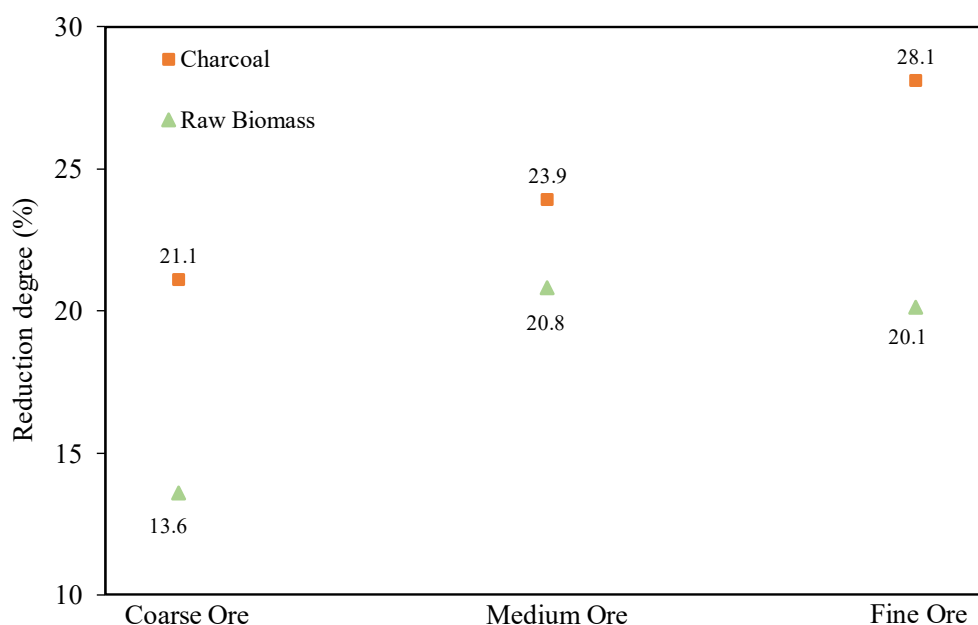
Figure 2.6. Reduction degree of iron ore in different particle sizes with pyrolytic gases from raw biomass and charcoal at 980 ºC.

It was observed that the finest particle size (-2.3+0.84 mm) resulted in the highest reduction degree, which reached 20.11% and 28.12% for raw biomass and charcoal, respectively. On the

other hand, as the particle size of the iron ore increased, the reduction degree decreased significantly. The smallest reduction degree (13.58%) was obtained for the coarse iron ore (-8.0+6.3 mm) and raw biomass, while for the coarse iron ore and charcoal, the reduction degree reached 21.10%. Concerning the medium iron ore particle size (-5.6+3.36 mm), when it was reduced by the pyrolytic gases from charcoal an intermediate reduction degree was obtained (23.93%), while the RD reached 20.79% for raw biomass.

The effect of particle size on the iron ore RD can be explained in terms of external and internal surface area. The smallest reduction degrees seen for all coarse-grained ores are associated with the smaller external surface area available for the superficial reduction and the greater diffusion resistance for the reducing gas species to access the particles' core [33,34]. Since the gas-solid reduction of the coarse iron ore is controlled by diffusion [35,36], increasing the diffusion path results in the greatest barrier to internal mass transfer. On the other hand, smaller grain size led to a greater surface area available for chemical reactions, in addition to shortening the diffusion path. Therefore, fine ores achieved higher reduction degrees.

Figure 2.6 also shows that ores with the same particle size presented lower reduction degrees when heated with raw biomass. This behavior is related to the different reducing atmospheres generated by each biomass since the composition of the reducing gas plays a major role in the gas-solid reduction behavior of iron oxides [36,37]. As shown in Figure 2.4, the main reducing gas available during the raw biomass pyrolysis was CO, while the reducing atmosphere provided by the charcoal pyrolysis was richer in H_2. Moreover, the reducing gases, mainly H_2, are released from charcoal at higher temperatures, which favors the reduction kinetics. Therefore, the smaller RD by raw biomass provides evidence that H_2 had a greater reducing potential when compared to CO. According to Yi *et al*. [23] and Zuo *et al*. [38], the fastest reduction rate occurs when H_2 is the major component in the gaseous mixture, while the lowest rate is obtained when CO is dominant. The latter is due to the higher diffusion capacity of H_2 and its superior adsorption on the iron oxide lattice, owing to hydrogen's lower viscosity and smaller molecule.

2.3.5. Microstructural Analysis

Due to the higher RD, only the fine ores had their microstructure before and after reduction investigated by field emission gun scanning electron microscopy and energy dispersive X-ray

spectroscopy (FESEM-EDS). Besides the samples after the reduction test carried out up to 980 ℃, additional samples from interrupted tests at 600 ℃ were evaluated. Microstructure identification aimed to clarify the morphology evolution of hematite particles when heated with both biomasses.

The microstructure of the raw iron ore in Figures 2.7a, b, and c, reveals a smooth surface, with no relevant cracks or pores. Increasing magnification from Figures 2.7a to c, the presence of prismatic and dense grains is clear, typical of hematite ores. Elemental maps are also shown in Figure 2.7d for Fe and O as major elements, that is in accordance with a chemical composition of iron ore, and some slag elements, *i.e*., Al, Si, Mn, and Mg.
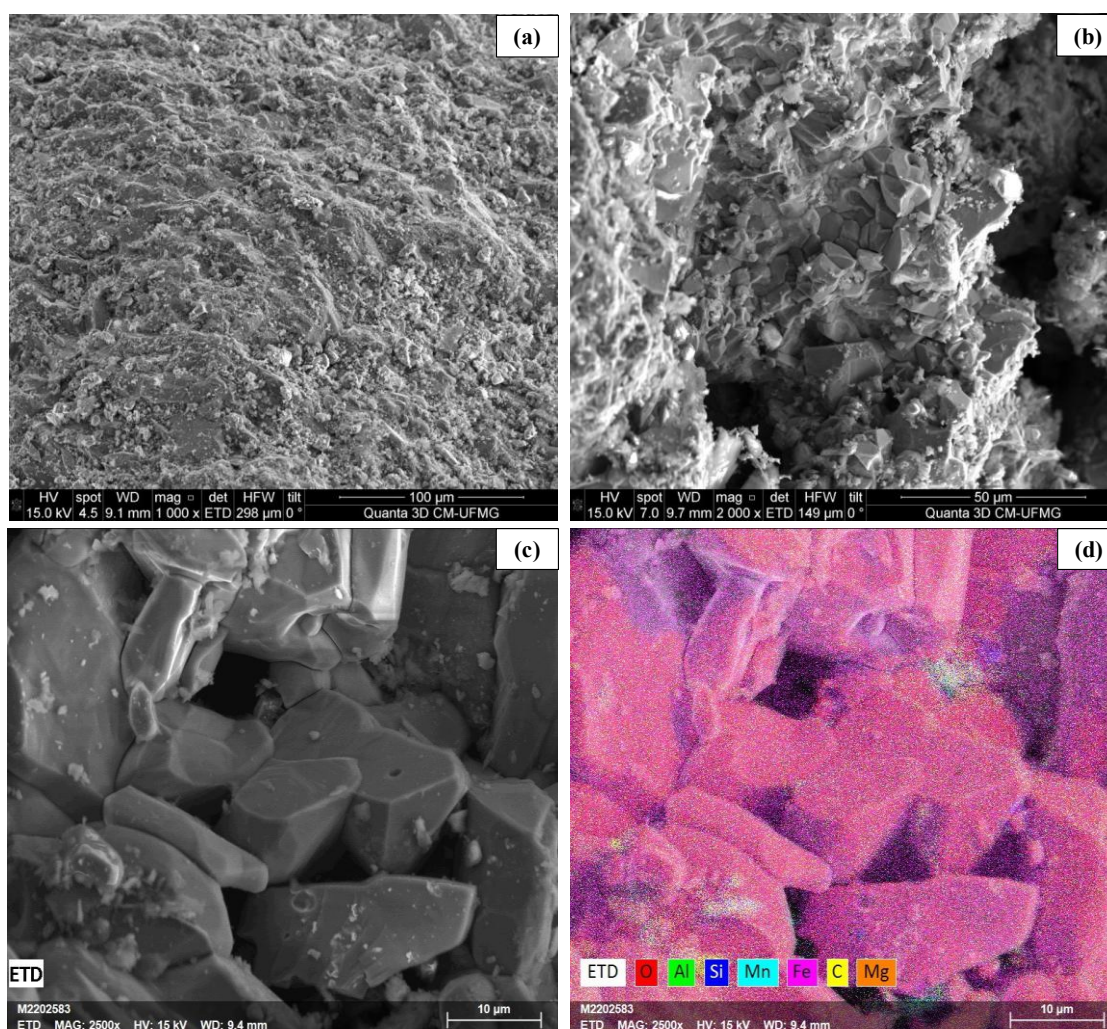
Figure 2.7. (a, b, and c) FESEM images and (d) EDS mapping of raw iron ore.

Figures 2.8a and b show the fine ore sample after interrupted experiments where the reaction occurred up to 600 ℃ with volatiles from raw biomass and charcoal, respectively. In the figures,

transgranular cracks (red arrows) are attributed to the volume expansion that is characteristic of the $Fe_2O_3 \rightarrow Fe_3O_4$ reduction step [39]. The hexagonal crystal structure of hematite is converted to magnetite with an equiaxed crystal structure, causing particle swelling and surface damage [40].
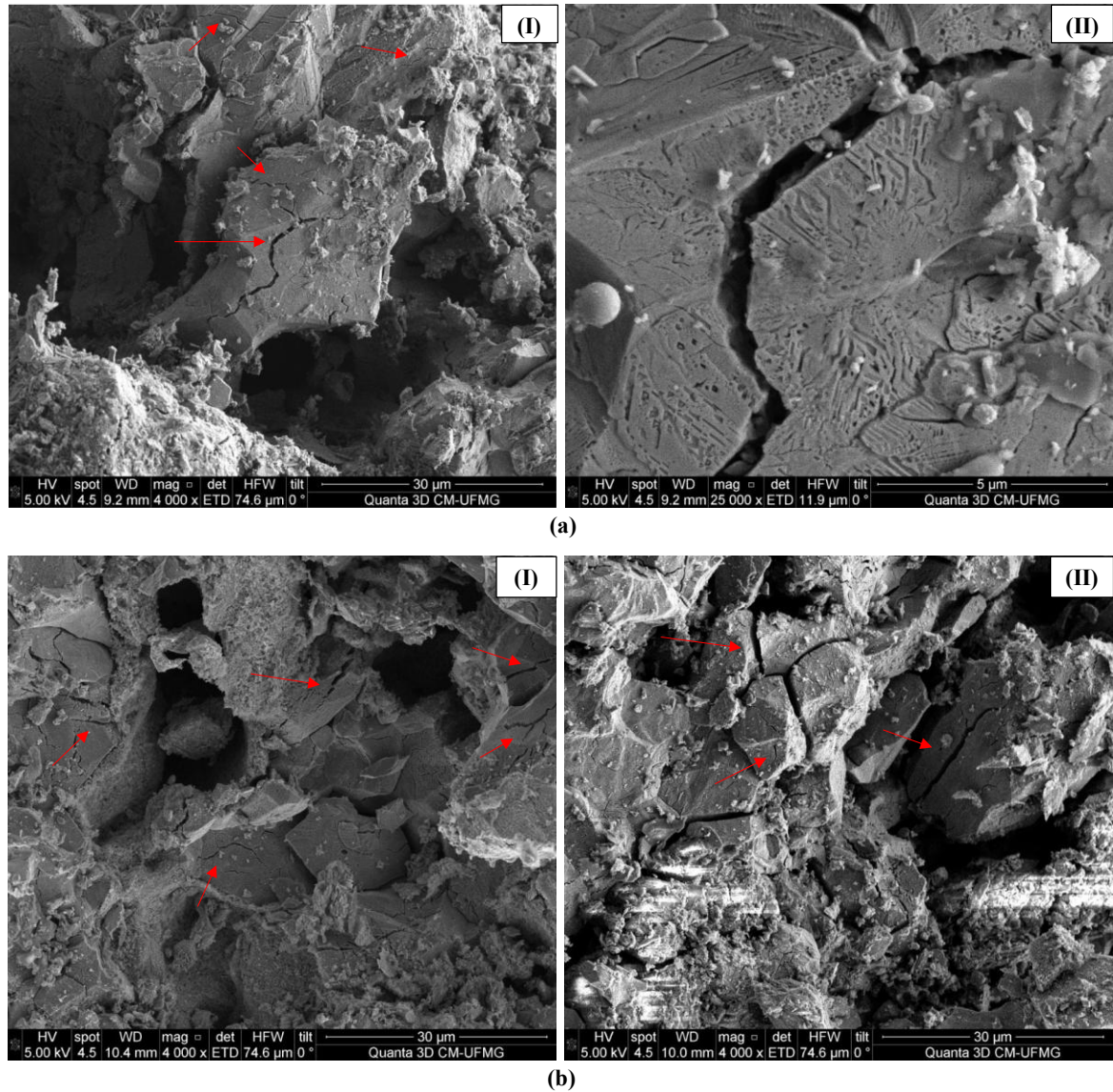
Figure 2.8. FESEM images of fine iron ore after heating with (a) raw biomass and (b) charcoal at 600 ºC.

XRD analysis was employed to identify iron compounds after interrupted tests at 600 ºC and the Rietveld analysis was used to quantify these phase fractions. It is observed in Figures 2.9a and b that for both biomasses, hematite is the major phase before and after reduction, although magnetite has been identified after tests. These results indicate that at 600 ºC, the type of

biomass used is indifferent to the progress of the reduction reactions, when more advanced stages of reduction are not targeted, and corroborates the partial reduction of the ore under these conditions, indicated by the presence of cracks in its morphology. In this context, the biomass volatiles were able to promote the partial magnetization of the ore, which is consistent with the morphological transformation observed in the FESEM images (Figure 2.8).
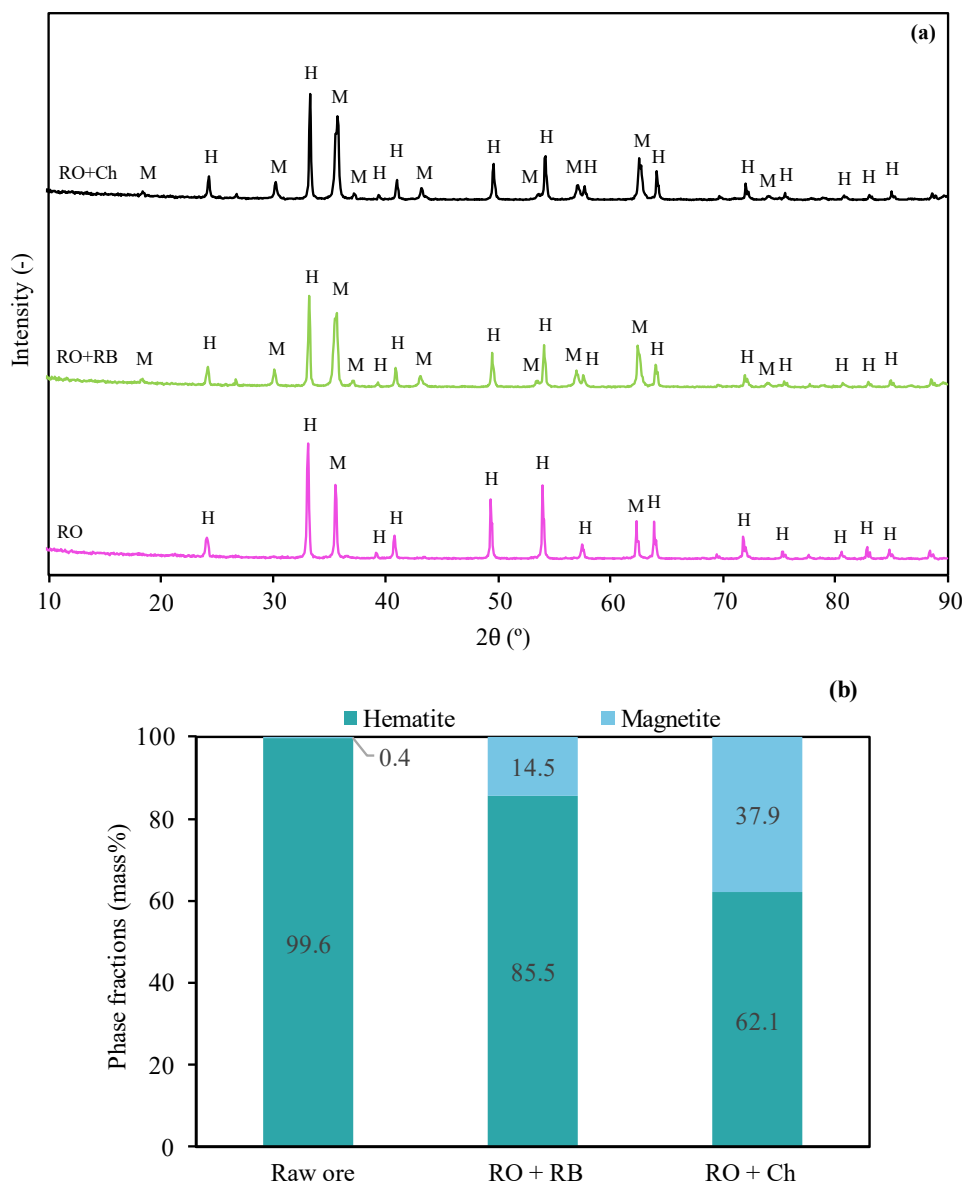
Figure 2.9. (a) XRD patterns of raw iron ore (RO) and fine ore heated with raw biomass (RB) and charcoal (Ch) at 600 °C, where H: hematite; M: magnetite; (b) phase fractions determined by the Rietveld analysis.

Figures 2.10a and b show the EDS analysis to identify carbon in the ore particles resulting from the interrupted tests at 600 °C, using raw biomass and charcoal, respectively. It was observed

that the ore particles resulting from the interrupted test with raw biomass presented a uniform distribution of C on their surface. These analyses also indicate that for raw biomass a uniform distribution of C throughout the iron ore can be seen, demonstrating that the deposition was more expressive than charcoal. This behavior was predicted because tar is generated in a temperature range from 400 to 700 ºC [25] and since charcoal has already been subjected to temperatures near that during its manufacture, tar release during charcoal devolatilization must be diminished. As mentioned in the previous studies in biomass pyrolysis, besides the non-condensable reducing gases, tar is also released, which can be deposited on the ore surface and catalytically crack, generating volatile matter and solid carbon. It is suggested that the formation of a uniform carbon layer on the ore surface ends up acting as a barrier between the reducing gases and iron oxide, limiting gas diffusion. This phenomenon hinders or even prevents the reduction progress, at least up to temperatures where the deposited carbon can be consumed, resulting in ores with low reduction degrees.
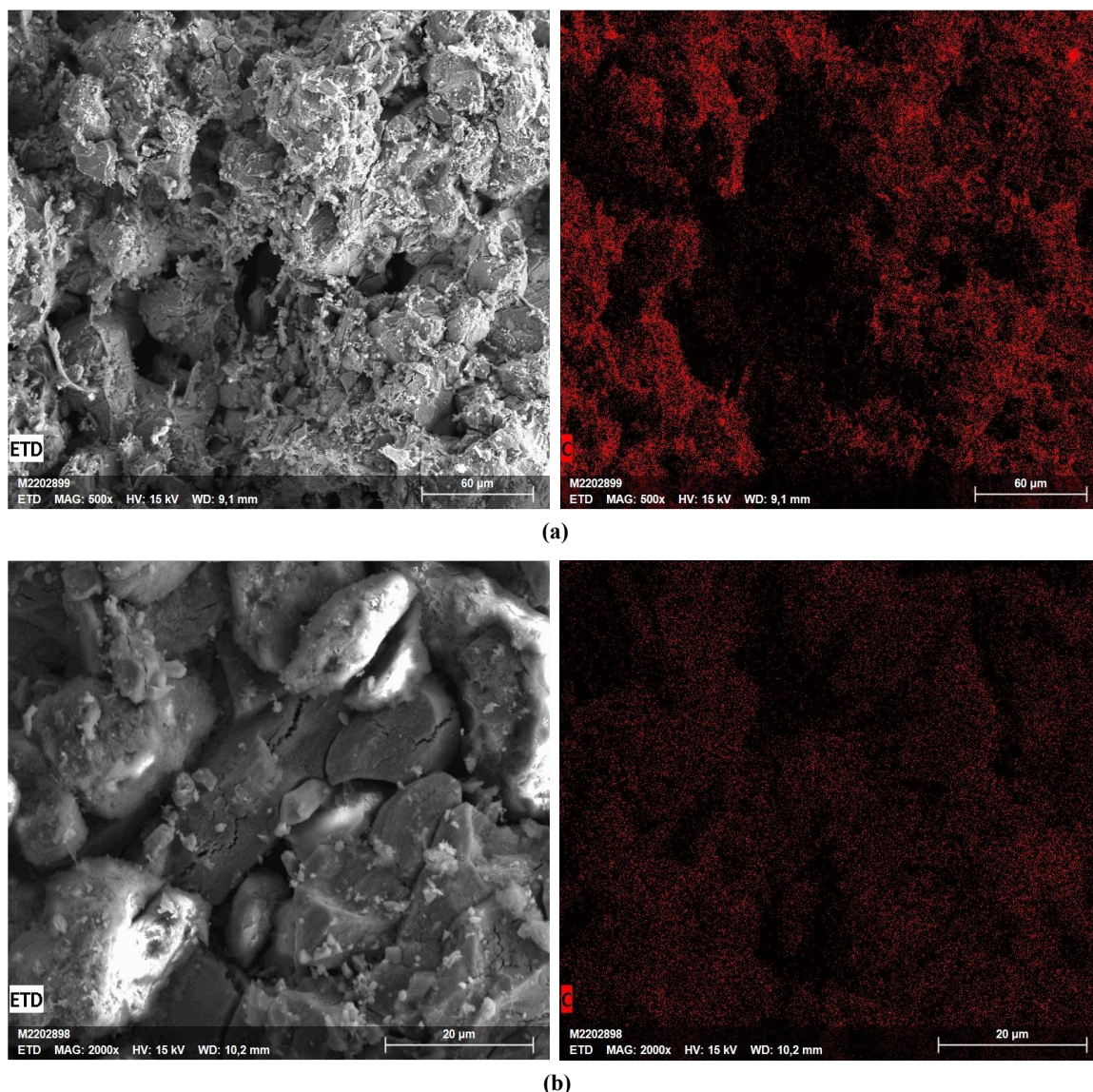
Figure 2.10. FESEM images and EDS carbon mapping of fine iron ore heated with (a) raw biomass and (b) charcoal up to 600 ℃.

Moreover, Figures 2.11a and b show the morphology of the products after heating with raw biomass and charcoal up to 980 ℃, respectively. Compared to samples interrupted at 600 ℃ (Figure 2.8), as the reaction advanced the ore's microstructure increased in porosity and microcracks. The pores and cracks present in magnetite facilitated the diffusion of the reducing gases inside the particle, promoting the advancement of the reducing reactions. The newly formed microstructure was enriched in porosity and microcracks, which indicates the predominance of the wüstite mineralogical phase [41,42]. Despite the clear presence of the wüstite microstructure, the XRD results (Figure 2.5), which show the presence of residual magnetite peaks, indicate that FeO was not formed throughout the ore particle, indicating that

the test time was insufficient for the reaction to occur in the inner layers of the particles. It is also worth noting that no significant amounts of metallic Fe nor the formation of whiskers were observed, according to the XRD and FESEM results, respectively.
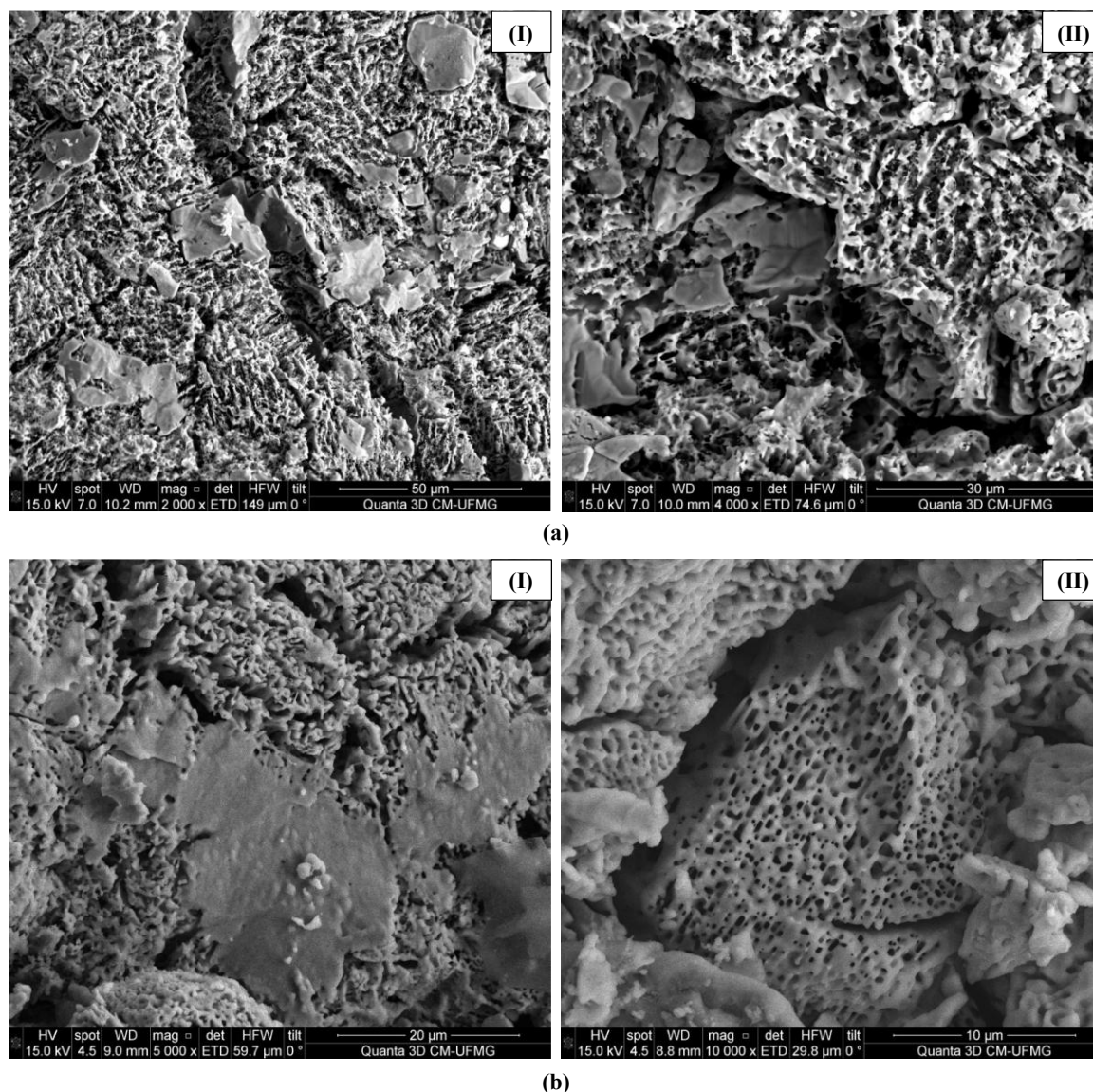
Figure 2.11. FESEM images of the fine ore after heating with (a) raw biomass and (b) charcoal at 980 °C.

Moreover, Figure 2.11 also shows the difference in the morphology of formed wüstite. In Figure 2.11a the structure formed by the reduced particles is less dense than that shown in Figure 2.11b, where a more compact structure can be seen. This morphological difference may be related to the reducing agent and to the temperature at which the iron ore reduction occurred. Figure 2.12 presents the FESEM-EDS images of the fine ore particle heated with raw biomass at 980 °C.

This analysis reveals that in the temperature range of 600-980 ºC, the carbon contained in the samples was significantly consumed. These results match with what was suggested from the gas analysis of this study, where the simultaneous increase in the CO and CO_2 flow rate is a consequence of the simultaneous occurrence of indirect reduction of iron ore (2.9), Boudouard reaction (2.10) and direct reduction between iron oxide and deposited solid carbon (2.11).

$$Fe_xO_{y(s)} + CO_{(g)} \rightarrow Fe_xO_{y-1(s)} + CO_{2(g)} \tag{2.9}$$

$$C_{(s)} + CO_{2(g)} \leftrightarrow 2CO_{(g)} \tag{2.10}$$

$$FeO_{x(s)} + C_{(s)} \rightarrow FeO_{x-1(s)} + CO_{(g)} \tag{2.11}$$
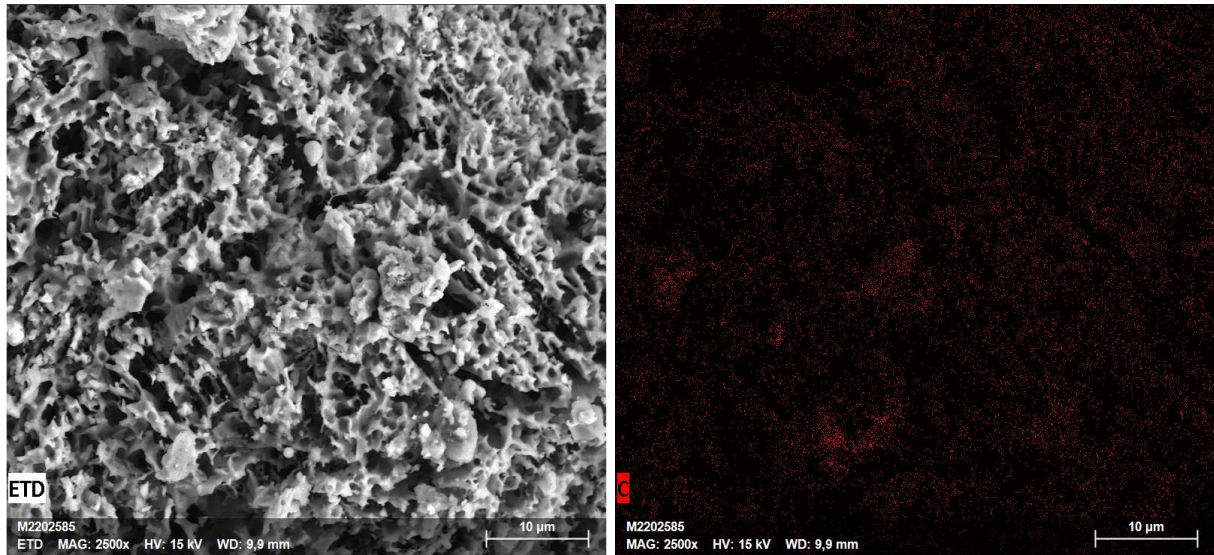
Figure 2.12. FESEM image and EDS carbon mapping of fine iron ore heated with raw biomass up to 980 ºC.

The reducing atmosphere generated by heating both biomasses was a mixture of CO and H_2. The CO/H_2 ratio was higher for the raw biomass pyrolysis with a maximum concentration of CO at about 500 ºC, while for the charcoal pyrolysis, the CO/H_2 ratio is lower and H_2 presents a maximum concentration close to 900 ºC. For the iron ore heated with charcoal, obtaining mostly wüstite and the highest global RD are related to the availability of the reducing gases, mainly H_2, at favorable temperatures for the higher iron oxides (Fe_2O_3 and Fe_3O_4) reduction. The resulting microstructure agrees with earlier predictions of John & Hayes [43], where these authors showed similar morphology for the wüstite reaction at H_2-rich atmosphere close to 900 ºC. In addition, according to XRD results (Figures 2.5b and c), iron ore passed predominantly the reduction stages of $Fe_2O_3 \rightarrow Fe_3O_4 \rightarrow FeO$ in H_2-containing gases. Therefore, the range of

the expansion state during reduction was narrowed and dense wüstite with fine pitting was significantly formed up to about 900 ºC. So, when heated with charcoal, H_2 was the main reducing agent of iron oxides.

However, the microstructure of the reduced product by raw biomass volatiles was visually less compact, and a rougher wüstite surface was observed. Previous reports have shown that as the reduction transformation temperature increases, the products become progressively less dense and more porous [39, 44]. According to Yi *et al.* [39], which evaluated the reduction of iron ore pellets at 800, 900, and 1000 ºC in H_2-CO mixtures, the swelling of agglomerates during reduction increase with temperature at CO atmosphere due to the mineralogical transformation of $Fe_3O_4 \rightarrow FeO$. For raw biomass, although a CO-H_2 atmosphere exists up to approximately 900 ºC, the porous wüstite was probably formed above this temperature, *i.e.*, close to 1000 ºC, due to the presence of deposited C.

The intimate contact of pyrolytic carbon with pre-reduced iron oxide particles contributed to an effective reduction and the morphological characteristics of the product. However, the reduction by non-condensable gases and solid C were not steps completely separated during heating and must happen simultaneously.

Regarding the different product microstructures produced by the different raw materials, it is expected that the two products will behave differently for further reduction. The last step of iron oxides reduction, that is the transformation of wüstite to metallic iron, it is the most important step of the reduction process and determines the overall reduction rate and the amount of reducing gas used. In gas-solid reactions, the morphological structure of the intermediate solid products plays an important role in the reduction kinetics. When diffusion is the rate-determining step of reduction and the internal specific area of the solid is high enough to participate in the reaction quickly, the necessary temperature can be significantly diminished [45]. Therefore, according to the two morphologies obtained, it is estimated that wüstite from the reaction of iron ore and raw biomass volatiles will have a faster reduction kinetics than that formed from charcoal volatiles since it has a higher surface area.

2.4. Conclusions

In this work, the reduction of hematite iron ore in three different particle sizes by volatiles from raw biomass and charcoal was investigated. When the ores were simultaneously heated with the biomasses up to 980 ℃, it was possible to observe a significant phase transformation, with wüstite being the major mineral. This transformation was more significant for fine ore heated with charcoal. During the pyrolysis of the biomasses with the fine ore up to 600 ℃, the volatiles did not provide a significant reduction of the hematite which was the major phase in the product. Deposition of carbon on the fine ore surface was observed, especially after heating with raw biomass. Electron microscopy analyses showed that this carbon was consumed in tests carried out up to 980 ℃. The variation in the wüstite morphology indicated that for the ore treated with raw biomass, deposited C was the main reducing agent, while for the product treated with charcoal, the reduction occurred mainly by H_2. Therefore, these results indicate that condensable and non-condensable volatiles from raw biomass and charcoal fines can become an alternative source of reducing agents, contributing to the reduction of fossil fuel consumption in the steel industry.

Acknowledgments

2.5. References

[1] World Steel Association (2021) Steel Statistics. https://www.worldsteel.org/steel-by-topic/statistics.html. Acessed: 28 January 2022.

[2] Suopajärvi, H.; Umeki, K.; Mousa, E.; Hedayati, A.; Romar, H.; Kemppainen, A.; Wang, C.; Phounglamcheik, A.; Tuomikoski, S.; Norberg, N.; Andefors, A.; Öhman, M.; Lassi, U.; Fabritius, T. (2018) Use of biomass in integrated steelmaking – Status quo, future needs and comparison to other low-CO_2 steel production technologies, Applied Energy 213:384-407.

[3] Wang, P.; Ryberg, M.; Yang, Y.; Feng, K.; Kara, S.; Hauschild, M.; Chen, W-Q. (2021) Efficiency stagnation in global steel production urges joint supply- and demand-side mitigation efforts. Nature Communications 12:2066.

[4] Strezov, V. (2006) Iron ore reduction using sawdust: Experimental analysis and kinetic modelling. Renewable Energy 31:1892–1905.

[5] Vassilev, S. V.; Vassileva, C. G.; Vassilev, V.S. (2015) Advantages and disadvantages of composition and properties of biomass in comparison with coal: An overview. Fuel 158:330–350.

[6] Deng, J.; Ning, X.; Shen, J.; Ou, W.; Chen, J.; Qiu, G.; Wang, Y.; He, Y. (2022) Biomass waste as a clean reductant for iron recovery of iron ore tailings by magnetization roasting. Journal of Environmental Management 317:115435.

[7] Piketty, M-G.; Wichert, M.; Fallot, A.; Aimola, L. (2009) Assessing land availability to produce biomass for energy: The case of Brazilian charcoal for steel making. Biomass and Bioenergy 33:180-190.

[8] Coleti, J.L.; Manfredi, G.V.P.; Vinhal, J.T.; Junca, E.; Espinosa, D.C.R.; Tenório, J.A.S. (2020) Kinetic investigation of self-reduction basic oxygen furnace dust briquettes using charcoals from different biomass. Journal of Materials Research and Technology 9:6:13282-13293.

[9] Lu, Z.; Chen, X.; Yao, S.; Qin, H.; Zhang, L.; Yao, X.; Yu, Z.; Lu, J. (2019) Feasibility study of gross calorific value, carbon content, volatile matter content and ash content of solid biomass fuel using laser-induced breakdown spectroscopy. Fuel 258:116150.

[10] Bagatini, M.C.; Kam, T.; Evans, T.J.; Strezov, V. (2021) Iron ore reduction by biomass volatiles. Journal of Sustainable Metallurgy 7:215–226.

[11] Ni, M.; Leung, D. Y. C.; Leung, M. K. H.; Sumathy, K. (2006) An overview of hydrogen production from biomass. Fuel Processing Technology 87:461-472.

[12] Guo, D.; Zhu, L.; Guo, S.; Cui, B.; Luo, S.; Laghari, M.; Chen, Z.; Ma, C.; Zhou, Y.; Chen, J.; Xiao, B.; Hu, M.; Luo, S. (2016) Direct reduction of oxidized iron ore pellets using biomass syngas as the reducer. Fuel Processing Technology 148:276-281.

[13] Cahyono, R.B.; Yasuda, N.; Nomura, T.; Akiyama, T. (2014) Optimum temperatures for carbon deposition during integrated coal pyrolysis–tar decomposition over low-grade iron ore for ironmaking applications. Fuel Processing Technology 119:272–277.

[14] Zulkania, A.; Rochmadi, R.; Cahyono, R.B.; Hidayat, M. (2021) Investigation into Biomass Tar-Based Carbon Deposits as Reduction Agents on Iron Ore Using the Tar Impregnation Method. Metals 11:10:1623.

[15] Sahu, S.N.; Meikap, B.C.; Biswal, S.K. (2022) Magnetization roasting of waste in ore beneficiation plant tailings using sawdust biomass; A novel approach to produce metallurgical grade pellets. Journal of Cleaner Production 343:130894.

[16] Sindifer (2022) – Union of the Iron Industry in the State of Minas Gerais. Statistical Yearbook – Reference 2021.

[17] Delatorre, F.M.; Cupertino, G.F.M.; Oliveira, M.P.; Gomes, F.S.; Profeti, L.P.R.; Profeti, D.; Júnior, M.G.; Azevedo, M.G.; Saloni, D.; Júnior, A.F.D. (2022) A Novel Approach to Charcoal Fine Waste: Sustainable Use as Filling of Polymeric Matrices. Polymers 14:24.

[18] Surup, G.R.; Kaffash, H.; Ma, Y.; Trubetskaya, A.; Pettersen, J.B.; Tangstad, M. (2022) Life Cycle Based Climate Emissions of Charcoal Conditioning Routes for the Use in the Ferro-Alloy Production. Energies 15:11.

[19] Silva, G.L.R.; Braga, E.M.H.; Assis, P.S.; Quintas, A.C.B.; Dornelas, P.H.G.; Moura, L.C.A.; Souza, R.D.S. (2016) Utilização de finos de carvão vegetal para produção de biocoque metalúrgico. 46º Seminário de Redução de Minério de Ferro e Matérias-primas, 17º Simpósio Brasileiro de Minério de Ferro e 4º Simpósio Brasileiro de Aglomeração de Minério de Ferro. ABM Week.

[20] Manera, C.; Perondi, D.; Barcellos, T.; Godinho, M. (2020) CO_2 gasification of elephant grass: Effect of Ni/mayenite catalyst on dry reforming of tar. Biomass and Bioenergy 143: 105829.

[21] Strezov, V.; Evans, T.J.; Hayman, C. (2008) Thermal conversion of elephant grass (*Pennisetum Purpureum Schum*) to bio-gas, bio-oil and charcoal. Bioresource Technology 99:8394–8399.

[22] Safdari, M-S.; Amini, E.; Weise, D.R.; Fletcher, T.H. (2019) Heating rate and temperature effects on pyrolysis products from live wildland fuels. Fuel 242:295–304.

[23] Yi, L.; Zhang, N.; Hao, H.; Wang, L.; Xiao, H.; Li, G.; Liang, Z.; Huang, Z.; Jiang, T. (2022) Synergetic conversion laws of biomass and iron ore for syngas and direct reduced iron co-production. Journal of Cleaner Production 363:132387.

[24] Sun, Y.; Liu, L.; Wang, Q.; Yang, X.; Tu, X. (2016) Pyrolysis products from industrial waste biomass based on a neural network model. Journal of Analytical and Applied Pyrolysis 120:94-102.

[25] Hata, Y.; Purwanto, H.; Hosokai, S.; Hayashi, J.; Kashiwaya, Y.; Akiyama, T. (2009) Biotar Ironmaking Using Wooden Biomass and Nanoporous Iron Ore. Energy & Fuels 23:1128-1131.

[26] Li, B.; Mbeugang, C.F.M.; Huang, Y.; Liu, D.; Wang, Q.; Zhang, S. (2022) A review of CaO based catalysts for tar removal during biomass gasification. Energy 244:123172.

[27] Sutton, D.; Kelleher, B.; Ross, J.R.H. (2001) Review of literature on catalysts for biomass gasification. Fuel Processing Technology 73:3:155-173.

[28] Oh, J.; Noh, D. (2017) The reduction kinetics of hematite particles in H_2 and CO atmospheres. Fuel 196:144–153.

[29] Wang, L.; Yang, Y.; Zhong, Q.; Li, Q.; Jiang, T. (2022) Gasification of pine sawdust via synergetic conversion using iron ore as a catalyst. Bioresource Technology 355:127240.

[30] Ghosh, D.; Roy, A.K.; Ghosh, A. (1986). Reduction of Ferric Oxide Pellets with Methane. Transactions ISIJ 26:186:193.

[31] Lee, D. (2015) Hydrogen production via the Kværner process and plasma reforming. In: (Ed.). Compendium of Hydrogen Energy: Elsevier, 2015. p.349:391.

[32] Yang, H.; Yan, R.; Chen, H.; Lee, D.L.; Zheng, C. (2007). Characteristics of hemicellulose, cellulose, and lignin pyrolysis. Fuel 86:1781-1788.

[33] Turkdogan, F.T.; Vinters, J.V. (1971) Gaseous Reduction of iron Oxides. Reduction of Hematite in Hydrogen. Metallurgical and Materials Transactions B 2:3175-3188.

[34] Kazemi, M.; Glaser, B.; Sichen, D. (2014) Study on Direct Reduction of Hematite Pellets Using a New TG Setup. Steel Research International 85:4.

[35] Abdelrahim, A.; Iljana, M.; Omran, M.; Vuolio, T.; Bartusch, H.; Fabritius, T. (2020) Influence of H_2–H_2O Content on the Reduction of Acid Iron Ore Pellets in a CO–CO_2–N_2 Reducing Atmosphere. ISIJ International 60:2206-2217.

[36] Scharm, C.; Küster, F.; Laabs, M.; Huang, Q.; Volkova, O.; Reinmöller, M.; Guhl, S.; Meyer, B. (2022) Direct reduction of iron ore pellets by H_2 and CO: In-situ investigation of the structural transformation and reduction progression caused by atmosphere and temperature. Minerals Engineering 180:107459.

[37] Luo, S.; Fu, J. (2015) Co-pyrolysis of biomass tar and iron ore fines for the production of direct reduced iron. Journal of Renewable and Sustainable Energy 7:043131.

[38] Zuo, H.; Wang, C.; Dong, J.; Jiao, K.; Xu, R. (2015) Reduction kinetics of iron oxide pellets with H_2 and CO mixtures. International Journal of Minerals, Metallurgy and Materials 22:688-696.

[39] Yi, L.; Huang, Z.; Jiang, T.; Wang, L.; Qi, T. (2015) Swelling behavior of iron ore pellet reduced by H_2–CO mixtures. Powder Technology 269:290-295.

[40] Kang, T.; Gupta, S.; Sahajwalla, V. (2007) Characterizing Swelling Behaviour of Iron Oxides during Solid State Reduction for COREX Application and their Implications on Fines Generation. ISIJ International 47:11:1590-1598.

[41] Nascimento, R.C.; Mourão, M.B.; Capocchi, J.D.T. (1997) Microstructures of Self-reducing Pellets Bearing lron Ore and Carbon. ISIJ International 37:11:1050-1056.

[42] Ghadi, A.Z.; Valipour, M.S.; Vahedi, S.M.; Sohn, H. Y. (2020) A Review on the Modeling of Gaseous Reduction of Iron Oxide Pellets. Steel Research International 91:1900270.

[43] Jhon, D.H.St.; Hayes, P.C. (1982) Microstructural Features Produced by the Reduction of Wüstite in H_2/H_2O Gas Mixtures. Metallurgical Transaction B 13B:117-124.

[44] Rist, A.; Moujahid, S.E. (1988) The Nucleation of Iron on Dense Wüstite: A Morphological Study. Metallurgical Transactions B 19B:787-902.

[45] Von Bogdandy, L.; Engell, H.-J. (1971). The Reduction of Iron Ores – Scientific Basis and Technology. Springer-Verlag Berlin Heidelberg GmbH, 1971.

3. ARTIGO B. SUGARCANE BAGASSE AND IRON ORE TAILINGS THERMOCHEMICAL CONVERSION TOWARDS SUSTAINABLE IRON RECOVERY WITH BIOGENIC CARBON AND HYDROGEN PRODUCTION

Manoel V. B. Gonçalves[a*]; João V. M. Rocha[a]; Ismael V. Flores[b]; Maurício C. Bagatini[a]

[a] *Ironmaking Processes Laboratory (LPS), Department of Metallurgical and Materials Engineering, Federal University of Minas Gerais (UFMG), Av. Antônio Carlos, 6627, Bloco 2 – Sala 2242, Escola de Engenharia, 31.270-901, Belo Horizonte - MG, Brazil*

[b] *Department of Metallurgical and Materials Engineering, Federal University of Rio de Janeiro (UFRJ), Av. Horácio Macedo, 2030, Cidade Universitária, Centro de Tecnologia, Rio de Janeiro, 21.941-598, Brazil*

*Corresponding Author

Abstract

The recovery of valuable chemical elements from industrial waste is essential for production processes' economic and environmental sustainability. The interaction between the iron ore tailings and sugarcane bagasse, both wastes, has the potential to provide a secondary iron source for future iron and steelmaking processes. This study evaluated the use of volatiles from sugarcane bagasse (SCB) and iron ore tailings (IOT) to the synergistic promotion of carbon deposition, H_2 production and conversion of weak magnetic iron oxides in strong magnetic iron phases. The experiments were carried out at 400, 600, 800, and 1000 ℃ with different SCB/IOT ratios under an N_2 atmosphere. In all tests, SCB and IOT were heated simultaneously in separate beds to prevent direct contact between the materials. The combination of 600 ℃ and higher SCB/IOT ratio resulted in a product with 96.7% magnetite, 98% magnetic fraction recovery, and 3.5% deposited carbon. The use of lower SCB/IOT ratio provided an increase in H_2 production. Regardless of the mass ratio, heating the IOT and SCB simultaneously up to 1000 ℃ led to significant mineralogical transformations, reaching reduced phases such as wüstite, fayalite and metallic iron, which impaired magnetic separation efficiency. The results indicate an alternative for recovering iron from IOT using biomass waste as a renewable reducing agent for the steel industry.

Keywords: Biomass volatiles; Iron ore tailings; Iron recovery; Catalytic cracking; Carbon deposition; Hydrogen

Graphical Abstract
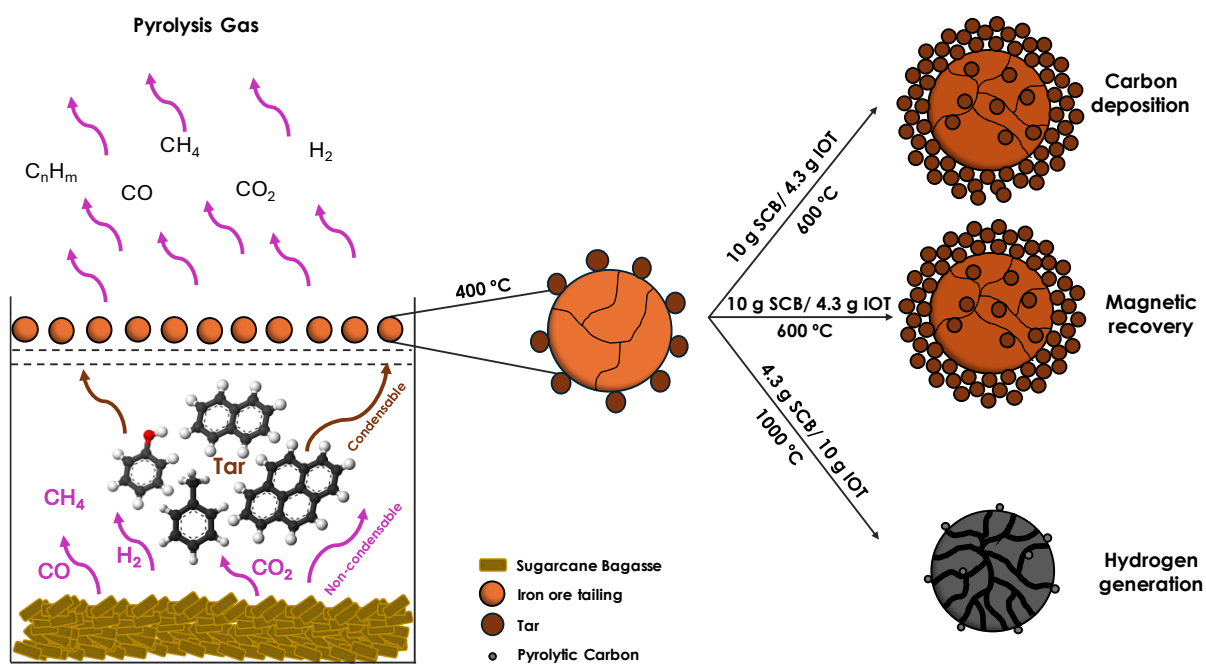
3.1. Introduction

The continuous increase in production of the steel industry, driven by the growing demand for these base materials, has contributed significantly to the development of modern society. The iron ore used for ironmaking requires mineral processing, which generates around 1.4 billion tons of iron ore tailings (IOT) annually worldwide. In Brazil, 260 – 275 million tons of IOT are generated and stored in tailing ponds yearly (Levandoski *et al*., 2023). On the other hand, the iron and steelmaking industry releases approximately 2.6 GtCO$_2$ annually, corresponding to 7-9% of all anthropogenic CO$_2$ (Kim *et al*., 2022).

Many studies have reported the development of methods for recycling the metals of interest from IOT. Iron recovery is particularly interesting because of its high concentration in this waste, and it is essential for the wide utilization of iron ore and the long-term development of the steelmaking industry (Deng *et al*., 2022; Dudchenko *et al*., 2024; Long *et al*., 2024). According to Carmignano *et al*. (2021) and Pinto *et al*. (2022), the Fe content of IOT typically ranges from 6 to 50%, and in certain instances, total Fe can exceed 60%. This iron is commonly found in the mineral form of hematite (α-Fe$_2$O$_3$) and goethite (α-FeOOH). Considering the global generation of IOT and the lowest iron content (6%), at least 84 million tons of metallic iron are wasted yearly. The methods mentioned for iron recovery include physical separation, flotation, and pre-reduction by magnetizing roasting of iron oxides (Qiu *et al*., 2023; Xu *et al*., 2024). Among these, studies have shown the effectiveness of magnetization roasting in the IOT concentration through the partial reduction of iron oxide by applying CO and H$_2$ as reducing agents (Dudchenko *et. al*., 2024; Zhang *et al*., 2019; Pinto *et al*., 2022).

Nevertheless, with increasing efforts from all industrial sectors to achieve net-zero emissions by 2050, developing strategies to decarbonize the iron and steelmaking industry is strongly required (Wang *et al*., 2021). Recent studies have highlighted biomass as a promising material for the steel industry's decarbonization in the near future. Biomass is available worldwide and is a renewable resource considered low-cost and neutral in terms of carbon emission. Moreover, biomass can be converted into solid, liquid and gaseous bioproducts through thermochemical processes, such as pyrolysis and torrefaction (Vassilev *et al*., 2015; Dhyani & Bhaskar, 2018). The raw biomass is majorly composed by volatile matter (70-75% by mass) (Bagatini *et al*., 2021) which from thermal processing is converted into non-condensable products, including CO, CO$_2$, H$_2$, and light hydrocarbons (such as CH$_4$), as well as condensable liquids such as tar

and oils (Ni *et al*., 2006). Using biomass as an energy and reducing agent source in ironmaking contributes to reducing the consumption of fossil carbon sources, such as coal and coke, thereby reducing net greenhouse gas emissions (Suopajärvi *et al*., 2017, 2018).

Magnetization roasting of iron ore tailings increases the difference in magnetism between the iron mineral and gangue, making it possible to convert weakly magnetic materials such as hematite and goethite into strongly magnetic magnetite, which is easily recovered in the magnetic separation process (Sun *et al*., 2019; Li *et al*., 2021; Qiu *et al*., 2023). Furthermore, depending on the conditions applied, oxidized ferrous phases can be converted into metallic iron. Sahu *et al*. (2022) assessed the iron recovery from iron ore tailings through magnetization roasting, employing sawdust biomass as a reducing agent. The experiments were conducted using mixed iron ore tailings and biomass in a muffle furnace. Their findings indicate that at 950 ºC and a residence time of 15 min with biomass yielded a high-grade magnetite concentrate with a Fe(T) content of 65.34%, suitable for metallurgical-grade pellet production. Deng *et al*. (2022) evaluated different biomasses (woody biomass and agricultural wastes of rice culture) as reducing agents for magnetization roasting in a lab-scale tube furnace. The authors showed that by combining woody biomass with IOT at 650 ºC, hematite was effectively converted to magnetite, promoting an iron recovery of 95.29% with a total iron content of 62.04%.

In the iron oxide reduction by biomass volatiles, iron oxides can be reduced by the synergistic effect related to the deposited tar, beyond the non-condensable gases from biomass decomposition (Bagatini *et al*., 2021; Gonçalves *et al*., 2024). As tar condenses on iron oxides, tar cracking catalyzed by iron minerals can occur, enriching the pyrolysis gases with valuable gas products, such as carbon monoxide and hydrogen, as well as carbon dioxide, methane, and other light hydrocarbons (Cahyono *et al*., 2014; Kurniawan *et al*., 2018). Nordgreen *et al*. (2012) showed that the composition and volume of gases, as well as the amount of deposited carbon, are partially controlled by the process temperature and oxidation state of the ferrous phase. Cahyono *et al*. (2014) determined the range of 400-600 ºC as the optimal temperature for coal pyrolysis-tar decomposition to obtain maximum carbon deposition on low-grade hydrated ores. Furthermore, the authors showed the ratio of tar to the catalyzing agent can be used to determine the amount of carbon deposition. Zulkania *et al*. (2021) demonstrated that a tar-iron ore ratio of 1.5 enhanced carbon deposition and the formation of carbon deposits on iron oxide accelerated the reduction rate as the temperature increased to 950 ºC. In addition to temperature, these authors showed that the ferrous phase, the ratio of catalytic and catalyzed

agents and the specific surface area of the ferrous source must be considered. The recovery of iron-containing deposited carbon from the simultaneous heating of iron ore tailings and biomass can provide an alternative raw material for self-reducing agglomerates. This method can enhance the efficiency of the steelmaking process and contributes to reducing CO_2 emissions, aligning with global carbon reduction targets.

Hydrogen is recognized as an alternative to mitigate air pollution and curbing greenhouse gas emissions (Cho *et al.*, 2024). However, hydrogen gas production using carbon-free energy, like biomass, is prohibitively expensive and low efficient, especially when the tar cracking process occurs by catalysts containing Pd, Pt, Ni, and Rh (Cahyono *et al.*, 2019). Increasing H_2 production from iron oxide-based catalyzed tar cracking might be an alternative route to produce green hydrogen and take advantage from the volatile matter produced in the biomass carbonization process.

This study examines two critical topics for industrial sustainability: the utilization of residual biomass in the steel industry and the mitigation of impacts associated with iron ore tailings storage. While the magnetization roasting of low-grade iron ore has been studied, there is a scarcity of data on continuous gas analysis, phase evolutions, and carbon deposition under varying experimental conditions, to improve the quality of solid and gaseous products resulting from the interaction between biomass volatiles and iron ore tailings in separate beds. This research aimed to evaluate different conditions that simultaneously enhance iron recovery, biogenic hydrogen production, and pyrolytic carbon deposition on the iron ore tailings by using sugarcane bagasse volatiles. Moreover, this study proposes an approach that allows for the use of volatiles generated during biomass thermochemical conversion processes for biocarbon production, a resource typically overlooked in conventional processes. This approach aligns with circular economy and decarbonization goals in the mining and metallurgical sectors.

3.2. Materials and methods

3.2.1. Raw materials

The iron ore tailings (IOT) were collected from the underflow fraction of the slurry thickener used in the iron ore beneficiation process. This material was obtained from an iron ore company located in the Quadrilátero Ferrífero, a mineral-rich province in the southeastern region of

Brazil. Before use, IOT was dried at 120 ºC, followed by disaggregation. Subsequently, the material was micropelletized using a pelletizing disc. The particle size distribution of the resulting IOT used in all the experiments is shown in Figure 3.1, where close to 70% of the particles range from 0.106-4 mm. Sugarcane bagasse (SCB) from a Brazilian sugar-ethanol company was used as source of biomass in all experiments and was used with a particle size below 2.38 mm. SCB was chosen as a renewable alternative compared to conventional fossil fuels.
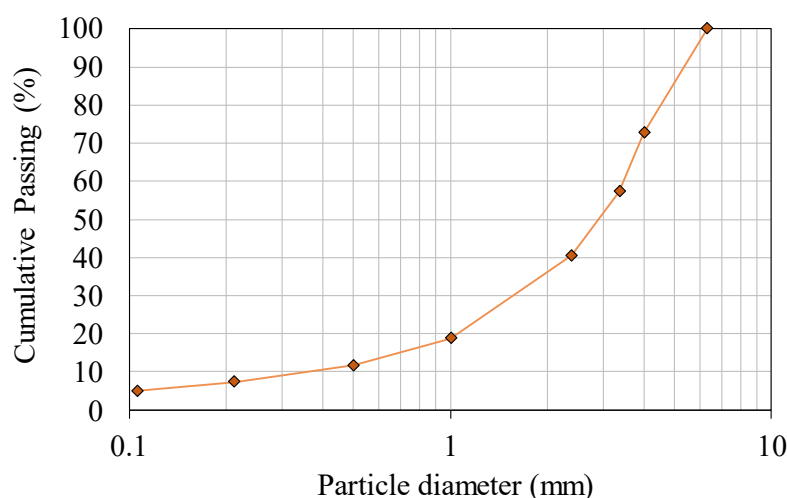
Figure 3.1. Particle diameter distribution curve of iron ore tailings micropellets.

The chemical composition of the iron ore tailing micropellets and biomass proximate analysis are presented in Tables III.1 and III.2, respectively. The chemical composition of the IOT was assessed using X-ray fluorescence spectroscopy (XRF), while the loss on ignition (LOI) was determined by measuring the mass loss of the samples upon heating in a muffle furnace at 1000 ºC for 1 h, according to ISO 11536:2015. The high LOI attributed to clay and goethite minerals as well as the elevated levels of silica and alumina (>12%), are the main challenges in upgrading the sample for suitable application in iron and steelmaking.

Table III.1. Chemical composition of iron ore tailing sample (weight %).

Fe_T	SiO_2	Al_2O_3	P_2O_5	K_2O	CaO	TiO_2	MnO	Na_2O	MgO	LOI[a]
51.12	5.39	7.00	0.60	0.06	0.12	0.46	0.29	0.03	0.92	10.77

[a] Loss on ignition

Table III.2. Proximate analysis of raw biomass (weight %).

Components (db[a])	Sugarcane bagasse
Volatile matter	77.56
Fixed carbon	18.6
Ash	3.84

[a]dry basis

3.2.2. Experimental

Two sets of experiments were conducted in this study. The first one evaluated the composition of gases emitted during biomass pyrolysis, while the second set explored the interplay between iron ore tailings and biomass volatiles to ascertain favorable conditions for carbon deposition, enhanced hydrogen production and magnetic recovery. A comprehensive description of the experimental procedure is provided following.

All tests were conducted in a vertical resistive furnace housing a stainless steel reactor tube, wherein the samples were heated within a graphite crucible. During the first set of experiments (pyrolysis-only), 10 g of dried SCB (105 ºC for 24 h) was heated at 10 ºC/min from room temperature up to 1000 ºC under a continuous flow rate of nitrogen of 1.5×10^3 Nml/min. Reaching 1000 ºC, an isothermal plateau was maintained for 15 min. The temperature in the experiments was continuously recorded using a furnace thermocouple. The released gases were passed through two condenser bottles (first containing room temperature water and the second containing water and ice) and then through an activated carbon filter for final purification. This setup ensured the removal of condensable gases and attained ambient atmospheric conditions, essential for accurate gas characterization by the gas analyzer. Continuous analysis was conducted using an Online Infrared Syngas Analyzer (Gasboard 3100 – Cubic Ruiyi).

In the second set of experiments (pyrolysis-reduction tests), SCB and IOT were simultaneously heated in separated beds, avoiding direct contact between both materials, but allowing the pyrolysis gases to flow through the IOT bed. Firstly, tests using 10 g of SCB and 10 g of IOT, at 400, 600, 800 and 1000 ºC, were simultaneously heated to evaluate the product yield and the composition of the gaseous fraction. To determine the favorable conditions for carbon deposition, hydrogen production and iron ore tailing magnetization the temperature (400; 600; 800; 1000 ºC) and biomass/iron ore tailings ratio (10 g/ 10 g; 10 g/ 4.3 g; 4.3 g/ 10g) parameters

were evaluated, and these conditions are presented in Table III.3. In all tests, the same heating and atmosphere conditions from the pyrolysis-only tests were employed and the resulting gas was also continuously analyzed. After the 15 min isotherm, the furnace was turned off and the samples were naturally cooled inside furnace in N_2 atmosphere.

Figures 3.2a and 3.2b shows a diagram of the experimental setup utilized in both test sets.
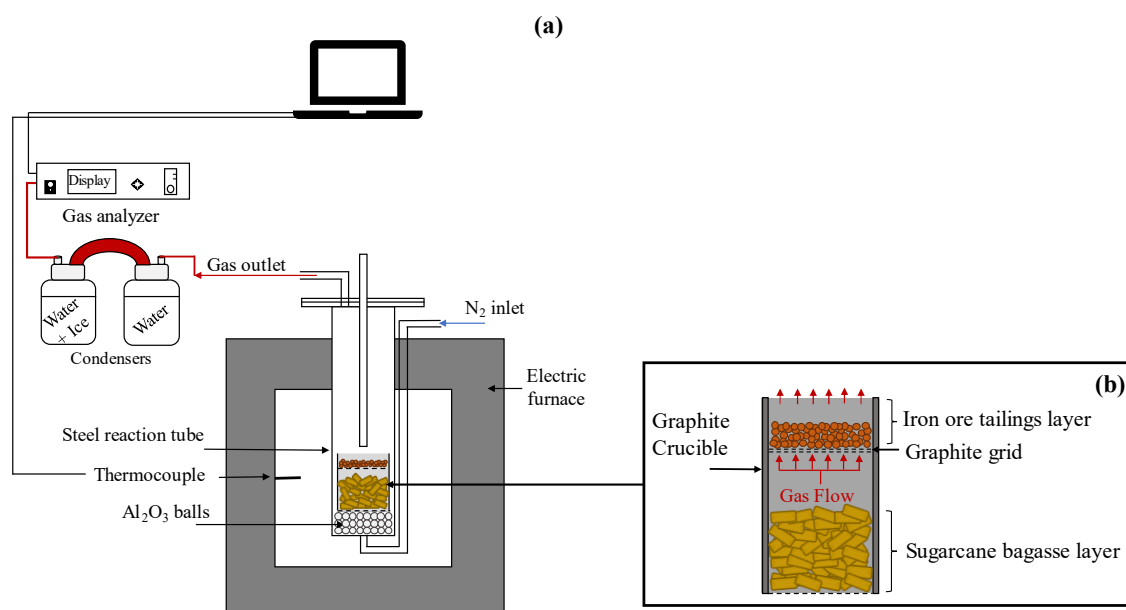
Figure 3.2. Diagram illustrating the experimental setup for pyrolysis and iron ore tailings reduction tests.

Table III.3. Variation of the experimental parameters employed in the simultaneous heating of sugarcane bagasse (SCB) and iron ore tailings (IOT).

Test		Maximum Temperature (°C)	SCB/IOT (g/g)
Base	SCB	1000	10/0
1	1.1	400	10/10
	1.2	600	10/10
	1.3	800	10/10
	1.4	1000	10/10
2	2.1	400	10/4.3
	2.2	600	10/4.3
	2.3	800	10/4.3
	2.4	1000	10/4.3
3	3.1	400	4.3/10
	3.2	600	4.3/10
	3.3	800	4.3/10
	3.4	1000	4.3/10

After the experiments, the IOT products were comminuted to a particle size of less than 53 μm, uniformly distributed on a flat surface, and subjected to high-field benchtop magnetic separation with magnetic field strength ranging from 1000 to 5000 Gauss distant in 40 mm. After this separation process, the percentage of mass recovered was calculated through the magnetized and non-magnetized mass fractions.

3.2.3. Phase analysis and carbon deposition

X-ray diffraction (XRD) analysis was used to identify the main mineral constituents of the iron ore tailings before and after the experiments. A Philips-PANalytical PW 1710 diffractometer was employed, using Cu (Kα) radiation and 2θ range from 3º to 80º, scan step size of 0.06º, acquisition time of 3 s, tube voltage of 50 kV, and current of 35 mA. Phase identification was carried out using X'pert High Score Plus software and the Rietveld method was applied to quantify the crystalline phases employing the same XRD software. The carbon content in the iron ore tailings was measured by an elemental analyzer (QCS - 1232, Quimitron).

3.3. Results and discussion

Following the pyrolysis products (only sugarcane bagasse and with iron ore tailings) are presented as well as the focused results concerning the synergistic performance on carbon deposition, H_2 production and magnetic recovery are discussed.

3.3.1. Pyrolysis products of sugarcane bagasse

The distribution of char, non-condensable (gas), and condensable products from biomass pyrolysis alone up to 1000 ºC are presented in Figure 3.3a. Figure 3.3b shows the non-condensable gases flow rates during the pyrolysis of sugarcane bagasse. The gas composition associated is shown in Figure 3.3c. These data of individual heating of biomass were assessed for subsequent comparison with experiments combining pyrolysis and iron ore tailings.
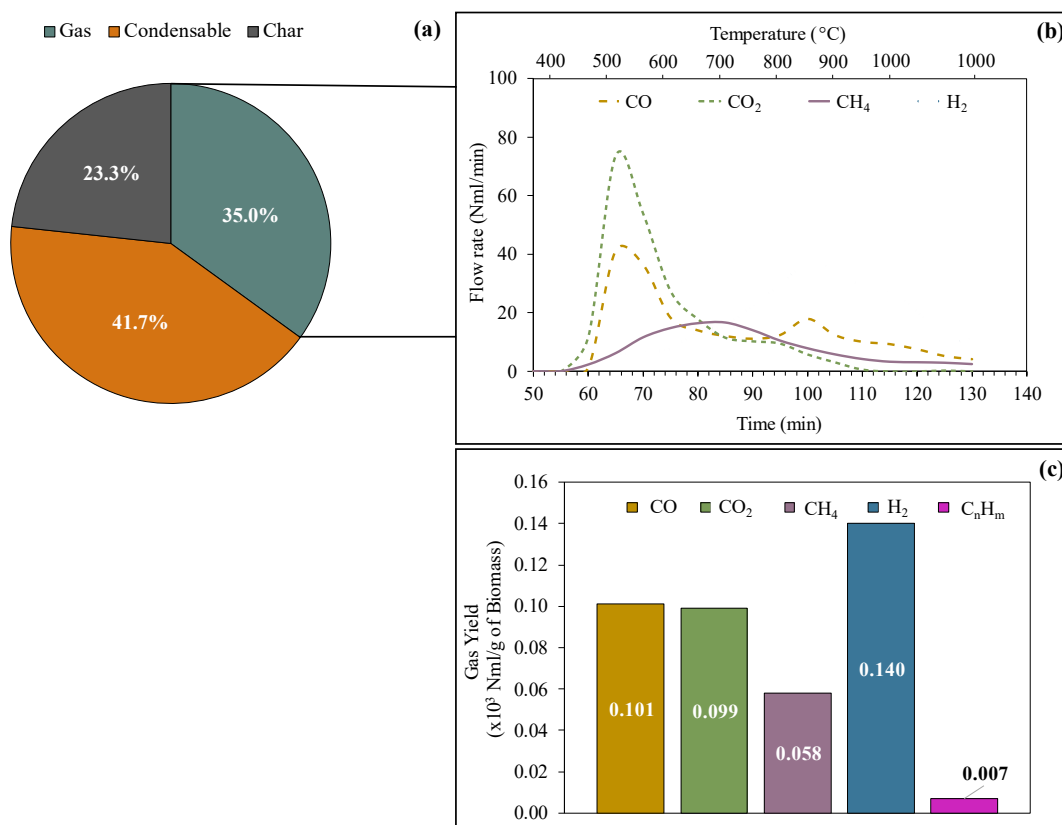
Figure 3.3. (a) Major products, (b) Gases release profile, and (c) Gaseous products composition from sugarcane bagasse pyrolysis up to 1000 ℃.

According to Figure 3.3a, pyrolysis of sugarcane bagasse resulted in 23.3% char, 41.7% condensable products, and 35% gaseous products. Lin & Kuo (2012) showed that in slow pyrolysis of sugarcane bagasse at 500 ℃ the char, condensable and gas yields were close to 36%, 47% and 17%, respectively. The lower yield of char and condensable products is associated with the fact that at temperatures above 600 ℃, bio-oils and char begin to be converted by secondary cracking reactions, increasing the gas yield (Uçar and Karagöz, 2009; Kan *et al*., 2016; Zhu *et al*., 2024).

Figures 3.3b and 3.3c shows the main gaseous products derived from the degradation of biomass structures (primary pyrolysis) and secondary reactions (secondary pyrolysis), which were CO, CO_2, CH_4, and H_2, with minor amounts of C_nH_m. According to Figure 3.3b, the initial detection of gaseous products from the sugarcane bagasse occurred at approximately 400 ℃. The maximum flow rates of CO and CO_2 were observed concurrently, peaking around 500 ℃. CH_4 showed a delayed peak, with maximum flow rate occurring at a higher temperature, approximately 650 ℃. In contrast, the flow rate of H_2 continued to increase, reaching its

maximum at approximately 850 ℃. The chemical composition of the gaseous products depends on the proportion and chemical structure of the biomass components, *i. e.* cellulose (25-50%), hemicellulose (15-40%), and lignin (10-40%) (Kan *et al.*, 2016; Kumar *et al.*, 2023). The amounts of CO (0.101×10^3 Nml/g of biomass) and CO_2 (0.099×10^3 Nml/g of biomass) shown in Figure 3.3c, were mainly associated with cellulose and hemicellulose degradation. During continuous slow heating process of biomass, cellulose and hemicellulose undergo thermal degradation (chain depolymerization) mainly up to approximately 400 ℃ (Shen *et al.*, 2010, Kan *et al.*, 2016). Nonetheless, differences in the initial detection of gases at lower temperatures can be attributed to the nature of the biomass and the pyrolysis conditions, such as heating rate, residence time, and system pressure. The production of hydrogen (0.140×10^3 Nml/g of biomass) and CH_4 (0.058×10^3 Nml/g of biomass), shown in Figure 3.3c, are mainly associated with the thermal depolymerization of lignin and its derivatives that occurs throughout the entire heating process and intensifies from 400 ℃ to approximately 1000 ℃. Moreover, the high hydrogen production shown in Figures 3.3b and 3.3c is due to the secondary thermal cracking of oils and reformation of the high-temperature vapor phase (Strezov *et al.*, 2008).

3.3.2. Yield of pyrolysis products with iron ore tailings

The products from the simultaneous heating of 10 g of sugarcane bagasse and 10 g of iron ore tailings at 400, 600, 800, and 1000 ℃ under a heating rate of 10 ℃/min, are shown in Figure 3.4.
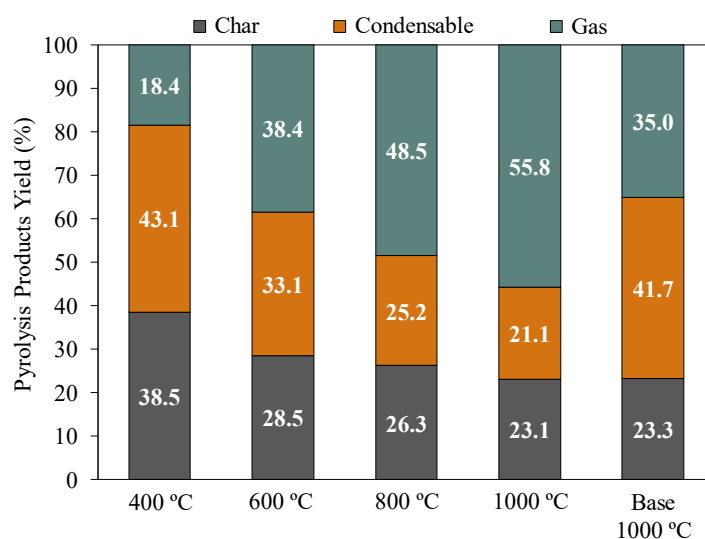

Figure 3.4. Products yield from sugarcane bagasse pyrolysis in the presence of iron ore tailings at different temperatures. Base is the pyrolysis carried out only with biomass.

As shown in Figure 3.4, when IOT and SCB were heated simultaneously, gases were already detected at 400 ºC. In contrast, as presented in Figure 3.3b of the previous section, SCB pyrolysis gases began to be detected at approximately 400 ºC. These variations are primarily attributed to the 15-minute isothermal plateau applied at each maximum temperature.

According to Figure 3.4, the impact of the temperature and the presence of IOT on the pyrolysis products was evident. As the temperature increased, there was a reduction in the solid product (char) and condensable (tar) yields, while there was an increase in the gaseous product yield. The higher percentage of gaseous products results from the thermal degradation reactions of biomass and char gasification. The yield of condensable products (tar) was also inversely proportional to temperature. According to Hata *et al*. (2009) and Li *et al*. (2022), tar is significantly released in the primary devolatilization of biomass from the pyrolysis/depolymerization of biomass components (cellulose, hemicellulose, and lignin) between 400 and 600 ºC. Efficient thermal tar cracking typically requires temperatures close to 1000 ºC (Sutton *et al*., 2001). However, in the presence of iron oxides, above 500 ºC, the primary tar condenses on the IOT particles and is catalytically cracked into solid carbon, non-condensable light gases (*i.e.* CO, CO_2, CH_4, and H_2) and hydrocarbons with lower molar masses (Reaction 3.1) (Bagatini *et al*., 2021; Zulkania *et al*., 2021). Metal oxides prevent the formation of stable chemical structures in hydrocarbons and accelerate hydrocarbon degradation by weakening C-C bonds, thereby reducing the activation energy required for the complex tar decomposition process (Cahyono *et al*., 2014).

$$\text{Tar} \xrightarrow{\text{Fe}_x\text{O}_y \ (\Delta)} H_2 + CO + CO_2 + CH_4 + C_{(s)} + \text{other light hydrocarbons} \qquad \text{(Reaction 3.1)}$$
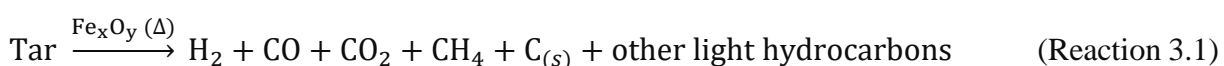
Notably, at 1000 ºC, the incorporation of IOT resulted in an increase in gaseous products and a decrease in condensable materials, while the char production remained nearly unchanged. This demonstrates the catalytic effect of iron oxides in breaking down condensable molecules, as previously mentioned. The use of IOT in industrial pyrolysis stations could serve as a filter for condensable materials, possibly reducing buildup in pipelines and enhancing both equipment lifespan and process productivity gas generation.

3.3.3. Gaseous products of pyrolysis with iron ore tailings

Figure 3.5a depicts the cumulative gas composition generated from 10 g of sugarcane bagasse pyrolysis in the presence of 10 g of iron ore tailings at four different temperatures. In Figure 3.5b, it is presented the mass ratio of CO_2/CO variation for such temperatures of heating.
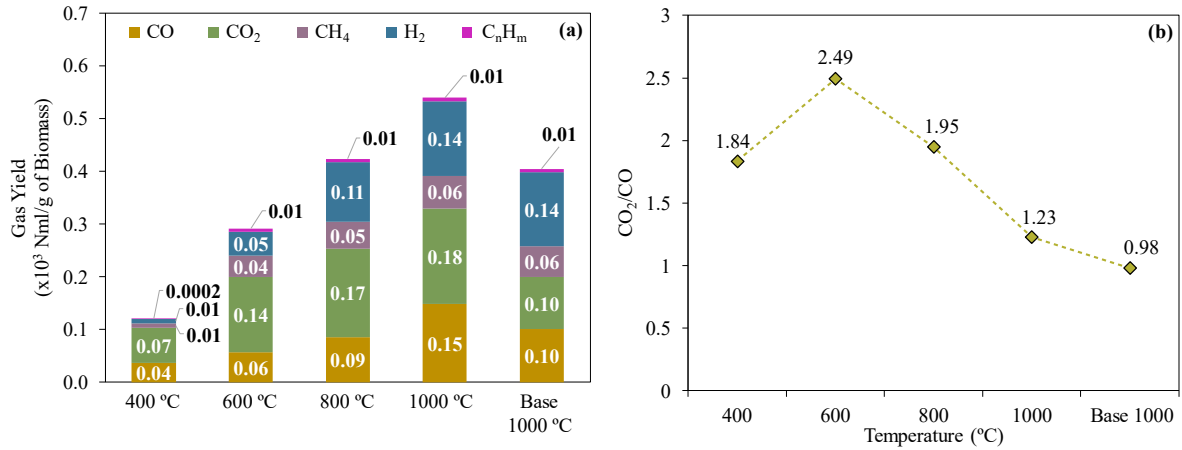
Figure 3.5. (a) Cumulative production of gaseous products from sugarcane bagasse during pyrolysis with iron ore tailings at four different temperatures with a heating rate of 10 ℃/min; (b) CO_2/CO relationship during the tests. Base is the pyrolysis carried out solely with biomass.

Considering only the test at 1000 ℃ and the base reference (solely biomass), notable increases were observed for CO_2 and CO owing to the presence of IOT. The increase in these two gas species indicates the occurrence of coupled gasification reactions (Boudouard reaction) (Reaction 3.2) of the deposited solid carbon in the IOT, as well as iron oxide reduction (Reactions 3.3) (Gonçalves *et al*., 2024).

$$C_{(s)} + CO_{2(g)} \rightarrow 2CO_{(g)}$$ (Reaction 3.2)

$$Fe_xO_{y(s)} + CO_{(g)} \rightarrow xFe_{(s)} + CO_{2(g)}$$ (Reaction 3.3)
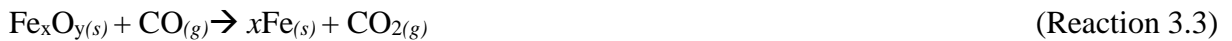
The more significant increase in CO_2 between 400 and 600 ℃, shown in Figures 3.5a and 3.5b, is related to the greater release of this gas from pyrolysis (Kumar *et al*., 2022), in addition to suggesting the occurrence of reduction reactions. On the other hand, the decrease in this relationship when increasing the temperature to 800 and 1000 ℃ (Figure 3.5b), made it evident that deposited carbon gasification, which generates CO, has become relevant in the iron ore tailing bed. However, this is not an isolated process, since the high reactivity to gasification of deposited carbon makes it a highly efficient reducing agent close to 800 ℃, which corroborates

the increase in CO_2 production. (Bagatini *et al*., 2021; Gonçalves *et al*., 2024). Furthermore, although the reduction of iron oxides through solid-state reactions (Reaction 3.4) is less favorable than reduction by gaseous agents, this reaction may also have contributed to the simultaneous increase of these two gases. It is worth noting that all CO_2/CO ratios obtained in the experiments combining SCB and IOT were higher than the baseline, indicating that reactions for the generation of CO_2 (mainly iron oxide reduction) were more significant than CO forming reaction, such as carbon gasification and tar cracking.

$$Fe_xO_{y(s)} + C_{(s)} \rightarrow Fe_xO_{y-1(s)} + CO_{(g)} + CO_{2(g)} \hspace{2cm} \text{(Reaction 3.4)}$$

At 1000 ℃ there was no variation in the overall H_2 production compared to the baseline. The most significant increase occurred when the temperature varied from 600 to 800 ℃, which is related to the temperature range in which H_2 is generated in greater quantities, mainly from lignin degradation and the occurrence of catalytic tar cracking (Yang *et al*., 2007; Gonçalves *et al*., 2024). Moreover, the H_2 participates in the reduction reactions (Reaction 3.5), since at high temperatures this gas is a very effective reducer due to thermodynamic (lower partial pressures required than CO) and kinetic (high gas diffusivity) aspects.

$$Fe_xO_{y(s)} + H_{2(g)} \rightarrow xFe_{(s)} + yH_2O_{(g)} \hspace{2cm} \text{(Reaction 3.5)}$$

Regarding CH_4, its variation was insignificant compared to the reference test, except at 400 ℃. According to Abbas & Daud (2010), thermal cracking of methane requires temperatures above 1200 ℃ owed to the strong C-H bonds. Although the use of a catalyst can significantly decreases the required temperature, the iron oxides from IOT were not efficient in catalytically cracking this molecule. Additionally, the iron oxide reduction by methane is complex and rarely occurs in one step within this temperature range (Ghosh *et al*., 1986). Therefore, the reduction kinetics driven by released biomass volatiles are faster than those of methane, making methane a reducing agent of secondary importance compared to carbon monoxide and hydrogen.

3.3.4. Analysis of H_2 generation and C deposition

Experiments with three proportions of SCB and IOT were conducted to investigate its effect on H_2 production and carbon deposition (Table III.3).

Firstly, the total gaseous production during the pyrolysis of sugarcane bagasse alone at 1000 ºC, as well as in the presence of IOT using different mass ratios at 400, 600, 800, and 1000 ºC, are presented in Figure 3.6.

Figure 3.6. Total gaseous production measured during simultaneous heating of SCB and IOT using different mass ratios and temperatures.

As shown in Figure 3.6, all tests indicated an increase in gas yield per gram of biomass rising temperatures, with the highest cumulative production occurring at 1000 ºC when using IOT. The gaseous yields between test 1 (10 g SCB/ 10 g IOT) and test 2 (10 g SCB/ 4.3 g IOT) did not show relevant changes at all temperatures. Conversely, at 400 ºC, the slightly higher total yield per gram of biomass in test 3.1, compared to tests 1.1 and 2.1, is attributed to the greater mass of IOT available to interact with the gases released during the primary devolatilization of biomass. Moreover, at 600, 800, and 1000 ºC, the highest gas productions per gram of biomass were achieved in tests using a lower ratio of SCB to IOT, *i.e*., in test 3 (4.3 g SCB/ 10 g IOT). Notably, the greatest variation in gas production occurred during the tests at 800 ºC.

Figure 3.7 shows the cumulative individual production of each gas after heating SCB with and without IOT at different mass ratios and temperatures.

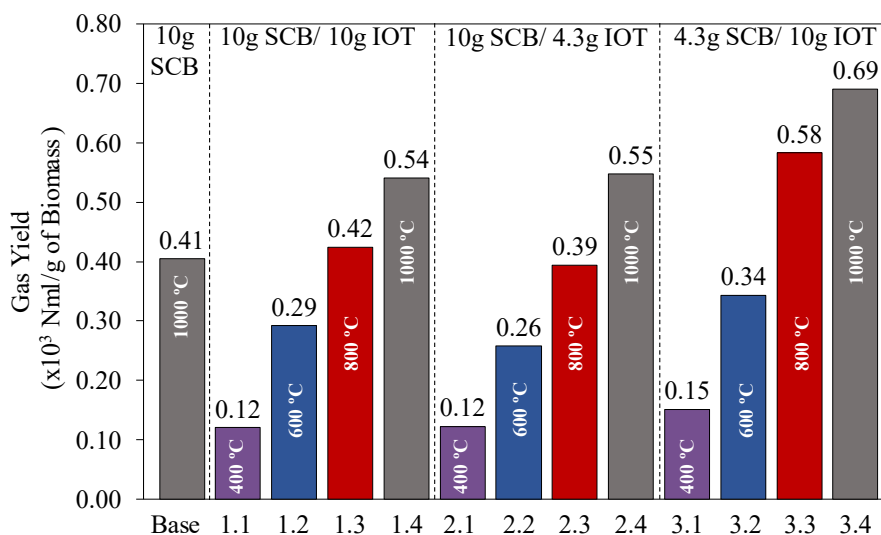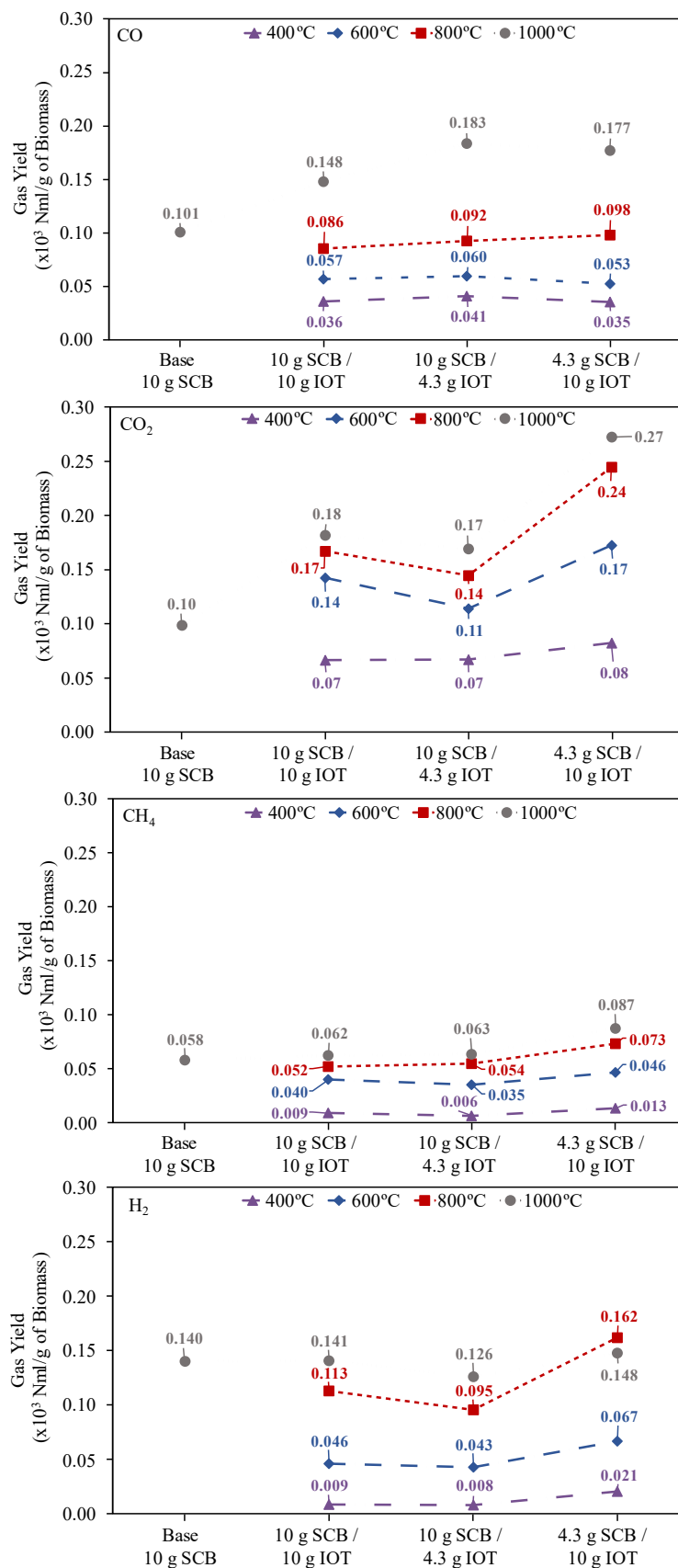**Figure 3.7.** Yield of individual gaseous species measured during simultaneous heating of SCB and IOT using different mass ratios and temperatures.

Taking test 1 (10 g SCB/ 10 g IOT) as a reference, according to Figure 3.7, at 600 ℃, there was an increase in H_2 production with less biomass (4.3 g SCB/ 10 g IOT - test 3), while higher SCB/IOT ratio (10 g SCB/ 4.3 g IOT - test 2) did not result in significant variation. At the same temperature, the CO_2 production decreased with higher SCB/IOT ratio (10 g SCB/ 4.3 g IOT - test 2) and increased with lower SCB/IOT ratio (4.3 g SCB/ 10 g IOT - test 3). Exceptions were CO and CH_4 whose production did not show significant changes. The increasing variation in the H_2 production is associated with the beginning of the tar catalytic cracking reaction, which was favored by a greater amount of IOT.

At 800 ℃, the H_2 production increased significantly with less biomass (4.3 g SCB/ 10 g IOT - test 3). Slightly higher CO and CH_4 production were obtained under the same conditions. These results indicate the advancement of tar catalytic cracking, favored by the greater amount of catalytic agent and higher temperature. Concerning CO_2, there was a production drop with higher SCB/IOT ratio (10 g SCB/ 4.3 g IOT - test 2) and a remarkable increase in lower SCB/IOT ratio (4.3 g SCB/ 10 g IOT - test 3). The increased production of H_2, CH_4, CO, and CO_2 in test 3.3 leads to the most significant variation in total gas production compared to the other tests at 800 ℃, corroborated by Figure 3.6. At 1000 ℃, the gas yields followed the same trend as that observed at 800 ℃, except for CO which compared to test 2 (10 g SCB/ 4.3 g IOT) showed a slightly lower yield when using less biomass (4.3 g SCB/ 10 g IOT - test 3).

Table III.4 presents the percentage changes in gas production for the three tests compared to the base. The variations indicate how different combinations of SCB and IOT affect the production of CO, CO_2, CH_4, and H_2 at 1000 ℃. In test 1 (10 g SCB/ 10 g IOT), the production of all gases increased, highlighting a 47% rise in CO and 84% rise in CO_2. In tests with higher SCB/IOT ratio (10 g SCB/ 4.3 g IOT - test 2), the production of CO, CO_2 and CH_4 followed the same trend, with CO production showing a significant 82% increase compared to the base. However, H_2 production in this test was 10% lower. Finally, in test 3 (4.3 g SCB/ 10 g IOT), even with a smaller amount of biomass, there was an increase in the production of all gases, highlighting a 76% rise in CO and 6% rise in H_2.

Table III.4. Variation of gas production ($x10^3$ Nml/g of biomass) at 1000 ºC.

Test	CO	CO_2	CH_4	H_2
Base: 10 g SCB	0.10	0.10	0.06	0.14
Test 1: 10 g SCB/ 10 g IOT	+ 47%	+ 84%	+ 7%	+ 1%
Test 2: 10 g SCB/ 4.3 g IOT	+ 82%	+ 71%	+ 9%	- 10%
Test 3: 4.3 g SCB/ 10 g IOT	+ 76%	+ 175%	+ 51%	+ 6%

Considering the higher ratio of SCB to IOT, a higher H_2 production was expected for test 2 (10 g SCB/ 4.3 g IOT). However, the variations in the hydrogen-generated volumes in these tests were smaller, possibly due to an excess of tar deposition in the IOT micropellets. This hypothesis indicates that the phenomena of the deposition and cracking of condensable matter and H_2 generation cannot be evaluated alone. In this context, Figure 3.8 graphically presents the results for the deposited carbon in the IOT.
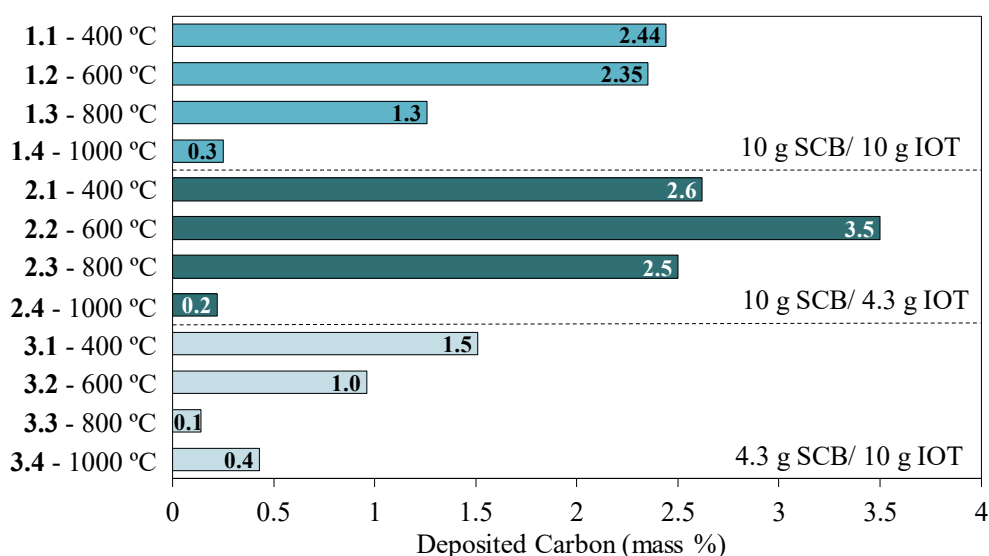
Figure 3.8. Deposited carbon on IOT particles during the pyrolysis and reduction process.

According to Figure 3.8, greater C content was observed under test 2 conditions (10 g SCB/ 4.3 g IOT), with the maximum deposition occurring in test 2.2 (600 ºC). The increase in the carbon content after treatment with higher SCB/IOT ratio (test 2), together with the reduction in hydrogen generation (Table III.4), suggests significant tar deposition on the micropellets' surfaces, but with less tar catalytic cracking. Effective catalysis by ferrous materials requires intimate contact between reactants. Successive layers of tar, resulting from excess mass of SCB to IOT, can hinder or deactivate the catalytic activity on the micropellets, hindering breakdown

reactions and gas formation, since the iron oxide surface area is the preponderant factor during the catalytic decomposition of biomass tar (Cahyono *et al*., 2019). Furthermore, the accumulation of tar can make it difficult for gaseous products from catalytic cracking to escape, making it difficult to renew the contact between tar and IOT. Thus, the similarity in the total volume of gases between test 1 and test 2 (Figure 3.6) can be attributed to the greater breakdown and tar gasification when a sufficient surface area is available on the IOT particles (10 g SCB/ 10 g IOT - test 1).

As shown in Figure 3.8, the carbon content in the micropellets decreased considerably at 800 and 1000 ℃ for all SCB/IOT ratios. This variation is attributed to the occurrence of carbon consumption by gasification and reduction reactions following the self-reduction mechanism (Bagatini *et al*., 2021; Gonçalves *et al*., 2024).

The conditions favoring carbon deposition on the IOT products occurred at 600 ℃ with higher SCB/IOT ratio (10 g SCB/ 4.3 g IOT (600 ℃) - test 2.2). Obtaining this Fe-C composite product can be particularly important for the reuse of iron ore tailings in iron and steel production processes as a raw material for self-reducing agglomerates. The intimate contact between deposited solid carbon on iron oxides (surface and pores) promotes the formation of Fe-C composites that behave as highly reactive self-reducing products. Owing to the nanoscale contact between iron oxide and carbon, the self-reduction reaction of this product begins at lower temperatures (750 ℃) than conventional self-reducing agglomerates composed by iron oxide and coke (1200 ℃), providing energy savings and reduced greenhouse gas emissions (Cahyono *et al*., 2014, 2019; Bagatini *et al*., 2021; Gonçalves *et al*., 2024).

Conversely, when the objective was to increase H_2 production, higher SCB/IOT ratio was not the best strategy, as intimate contact between the catalyst and the material to be catalyzed proved to be crucial to maximize the volumetric yield of this product. Under the tested conditions, the most relevant increase in H_2 production occurred for a smaller SCB to IOT amount (4.3 g SCB/ 10 g IOT - test 3), providing a greater surface area available for satisfactory tar catalysis. Thermochemical conversion is the most prevalent method for hydrogen generation from biomass (Lanjekar *et al*., 2023). However, hydrogen is preferentially released at high temperatures, which requires significant amounts of energy and increases costs.

3.3.5. Iron oxide conversion

Figures 3.9a, 3.9c, and 3.9e show the phases identified by X-ray diffraction (XRD) in the IOT before and after heating with different SCB/IOT ratios at different temperatures, while the respective Rietveld quantitative analysis are presented in Figures 3.9b, 3.9d, and 3.9f.
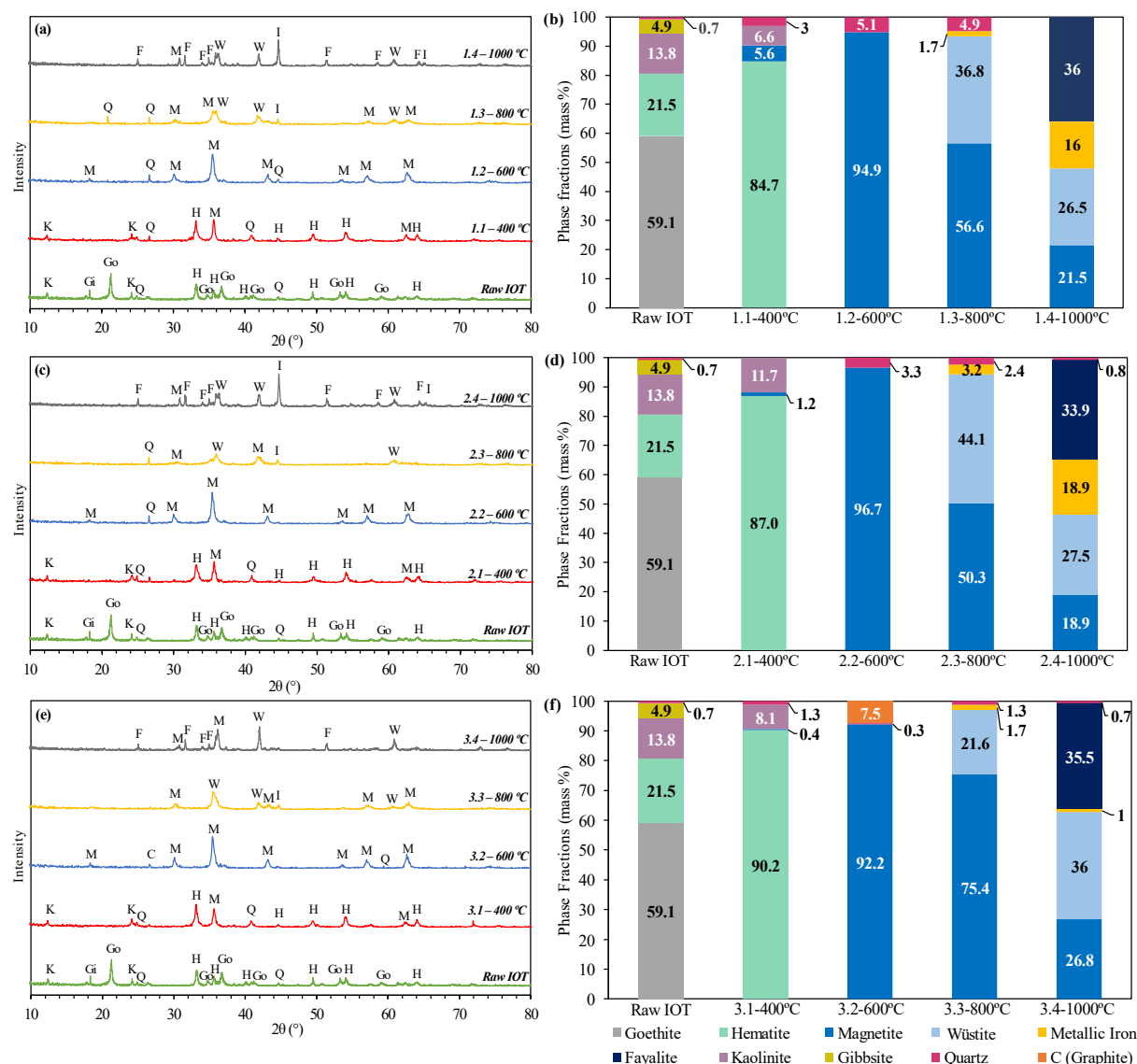
Figure 3.9. (a), (c), (e) XRD patterns and (b), (d), (f) Phase fractions determined by the Rietveld analysis of raw iron ore tailing and after heating with sugarcane bagasse, at 400, 600, 800, and 1000 ºC, with 10 g SCB/ 10 g IOT – test 1; 10 g SCB/ 4.3 g IOT – test 2; and 4.3 g SCB/ 10 g IOT – test 3, where Go: goethite; H: hematite; M: magnetite; W: wüstite; I: metallic iron; F: fayalite; K: kaolinite; Gi: gibbsite; Q: quartz; C: C-graphite.

Figure 3.9 reveals goethite (59.1%) and hematite (21.5%) as ferrous phases in raw IOT. In addition, kaolinite (13.8%), gibbsite (4.9%), and quartz (0.7%) were detected as secondary phases. The major presence of goethite agrees with the high LOI value for IOT (Table III.1).

After the tests at 400 ºC, the predominant crystalline phase was hematite, as all goethite transformed into hematite between 200 and 400 ºC (Reaction 3.6) (Naono *et al*., 1987; Ammasi, 2020). Additionally, the initial formation of magnetite was detected in all tests, especially in test 1.1. The partial occurrence of the first stage of hematite reduction ($Fe_2O_{3(s)} \rightarrow Fe_3O_{4(s)}$) was promoted at the beginning of biomass devolatilization, which supplied CO for the reaction medium.

$$2\alpha FeOOH_{(s)} \rightarrow \alpha Fe_2O_{3(s)} + H_2O_{(g)} \hspace{4cm} \text{(Reaction 3.6)}$$

At 600 ºC the main phase identified was magnetite. This result indicates that the gaseous products of SCB pyrolysis at this temperature have sufficient reducing potential to promote the formation of this mineralogical phase. The absence of kaolinite is explained by the fact that this temperature provides sufficient energy for the complete calcination of this clay mineral and the meta kaolinite formation, which depends on the clay mineral structure and is typically completed between 450 – 700 ºC (Ptáček *et al*., 2014). At 800 ºC, wüstite and metallic iron were detected, although magnetite remained the predominant ferrous phase.

At 1000 ºC, except in test 3.4, the magnetite and wüstite contents decreased further, with a consequent increase in the metallic iron content, in addition to the formation of fayalite (Fe_2SiO_4). During the reduction process, due to the relatively slow wüstite reduction to metallic iron, fayalite is formed when there is SiO_2 in the solid reactant, through Reaction (3.7). The formation of this phase is not desirable during the reduction processes due to its low reducibility, which will result in iron loss in the magnetic separation recovery processes (Zhong *et al*., 2020).

$$2FeO_{(s)} + SiO_{2(s)} \rightarrow Fe_2SiO_{4(s)} \hspace{4cm} \text{(Reaction 3.7)}$$

Figure 3.9 indicates that the biomass dosage influenced the proportion of the phases formed. Although test 2.2 showed a slightly greater production of magnetite, the similarity of this phase amount with tests 1.2 and 3.2 indicates that even a smaller amount of reducing agent promotes

the transformation to magnetite. This suggests that in tests 1.2 and 2.2 there was an excess of reductant. Even for a ratio of 4.3 g SCB/ 10 g IOT (test 3.2), there was sufficient reductant to convert all the hematite to magnetite. The mineralogical transformation of goethite led to the formation of pores in the micropellets (Cahyono *et al*., 2019; Zulkania *et al*., 2021). This enhanced the penetration of volatile matter from the SCB, facilitating the mass transfer between Fe_2O_3 and the reducing agent, thereby promoting the reduction process. This result is fundamental to optimizing the pre-reduction process as it reduces biomass consumption, costs and environmental impact. On the other hand, the over-reduction of hematite to form wüstite, in tests at 800 °C poses a substantial challenge to effectively recover iron from IOT, as this is a paramagnetic phase.

The influence of the amount of SCB on metallic iron formation was evident, as higher proportions were obtained with higher SCB/IOT ratios. Achieving an ideal balance between temperature and biomass amount is essential for maximizing the reduction process yield and metallic iron formation. However, at 1000 °C, although the Fe^0 content is high, the mineralogy of the product can be an inconvenience, as the presence of fayalite is undesirable in ironmaking processes.

3.3.6. Iron recovery by magnetization

The effects of the SCB/IOT ratios and temperature on the product magnetism after the reaction were explored and the results are presented in Figure 3.10.
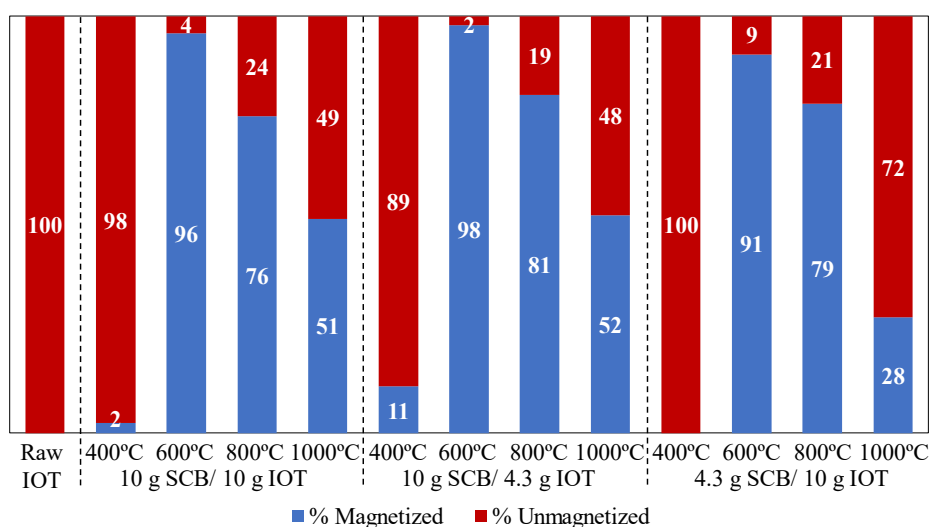

Figure 3.10. Magnetic separation from iron ore tailings after heating with sugarcane bagasse.

As shown in Figure 3.10, for the untreated material, no mass fraction was recovered through magnetic separation, owing to its weak magnetism. Magnetized fraction remained low for materials heated at 400 °C, reaching a maximum of 11% in test 2.1. The highest magnetic recovery was achieved at 600 °C, which is consistent with the highest magnetite content (Figure 3.9). Tests 1.2, 2.2, and 3.2 rendered magnetic fractions of 96%, 98%, and 91%, respectively. At 800 °C, the decrease in magnetic recovery can be attributed to over reduction and the formation of paramagnetic wüstite. Finally, a significant decrease in magnetic recovery was observed at 1000 °C. Therefore, the potential of thermochemical treatment to enhance magnetic fractions recovery from IOT is clear, and the magnetic properties of the materials varied significantly with different heating temperatures.

The variation between tests 1.4 and 2.4 was minimal, attributable to the mineralogical similarity of the products. Furthermore, it is worth mentioning that fayalite had a secondary influence on magnetic recovery from the three products. In contrast, magnetic recovery decreased significantly for the product treated with lower SCB/IOT ratio (test 3.4). Although this product had a higher percentage of magnetite, the lower content of Fe^0 (1%) probably had a major influence on the magnetic separation process.

Finally, it is shown that, in the conditions tested, 600 ºC is the temperature that favors the magnetization and consequent iron recovery from iron ore tailings. At this temperature and conditions, were formed products that allowed more than 90% magnetized fraction. Moreover, increasing the biomass ratio (10 g SCB/ 4.3 g IOT), promoted reaching up to 98% magnetizing fraction recovery, which maximizes iron recovery.

3.4. Conclusion

This study explored the synergistic processing of iron ore tailings (IOT) and volatiles from sugarcane bagasse (SCB) to enhance their value through iron recovery, hydrogen generation and carbon deposition. The interaction between SCB volatiles and IOT resulted in increased total gas production compared to biomass-only treatment, with higher temperatures (up to 1000 ºC) yielding greater gas volumes across all SCB/IOT ratios. Notably, the highest gas yields (Nml/g of biomass) were achieved with the lowest SCB/IOT ratio (4.3 g SCB/ 10 g IOT) at all evaluated temperatures.

Significant variations in the gaseous products from SCB-IOT interactions occurred at 1000 ºC, especially for H_2, CH_4, and CO_2. Hydrogen and methane production were primarily driven by effective catalytic tar cracking, and the lowest SCB content (4.3 g SCB/ 10 g IOT) enhanced H_2 production by 6% at 1000 ºC. In contrast, maximum carbon deposition (3.5%) on IOT micropellets was observed when 10 g SCB/ 4.3 g IOT was heated up to 600 ºC, indicating substantial tar deposition but limited catalytic tar cracking. These findings emphasize the importance of close interaction between the catalyst (iron phases) and deposited tar for effective tar catalytic cracking.

At 600 ºC, magnetite was the predominant phase across all SCB/IOT mass ratios, with a magnetite peak (96.7%) and magnetic recovery (98%) observed for 10 g SCB/ 4.3 g IOT. At 800 ºC, magnetic recovery decreased due to over-reduction, with paramagnetic wüstite formation reducing magnetic recovery to a minimum of 76% for 10 g SCB/ 10 g IOT. Simultaneously heating of IOT and SCB up to 1000 ºC induced significant phase transformations, forming reduced phases like wüstite, metallic iron and fayalite. Biomass proportion played a key role in metallization, with a higher biomass ratio (10 g SCB/ 4.3 g IOT) achieving 18.9% of metallic iron. By 1000 ºC, the magnetic recovery differences between the 10 g SCB/ 10 g IOT and 10 g SCB/ 4.3 g IOT ratios were minimal, due to mineralogical similarities. However, with 4.3 g SCB/ 10 g IOT, the metallic iron content was only 1%, and magnetic recovery significantly declined to 28%, indicating that metallic iron content substantially impacted the magnetic separation process.

These findings propose a technically feasible strategy to valorize iron ore tailings by utilizing sugarcane bagasse volatiles, effectively combining two industrial by-products. Additionally, they help mitigate environmental impacts while integrating renewable and sustainable sources of hydrogen and carbon, key components for ironmaking and the industry`s transition to zero-emissions. By doing so, this work promotes circular economy practices, contributes to greenhouse gas emission reductions, and supports the transition towards more sustainable industrial processes.

3.5. Reference

Abbas, H. F., Daud, W.M.A.W., 2010. Hydrogen production by methane decomposition: A review. International Journal of Hydrogen. 35,1160-1190.

Ammasi, A., 2020. Effect of Heating Rate on Decomposition Temperature of Goethite Ore. Transactions of the Indian Institute of Metals. 73,1,93-98.

Bagatini, M.C., Kan, T., Evans, T.J., Strezov, V., 2021. Iron ore reduction by biomass volatiles. Journal of Sustainable Metallurgy. 7,215–226.

Cahyono, R.B., Yasuda, N., Nomura, T., Akiyama, T., 2014. Optimum temperatures for carbon deposition during integrated coal pyrolysis–tar decomposition over low-grade iron ore for ironmaking applications. Fuel Processing Technology. 119,272–277.

Cahyono, R.B., Mansor, M.b., Nomura, T., Hidayat, M., Budiman, A., Akiyama, T., 2019. Steam Reforming of Tar Using Low-Grade Iron Ore for Hydrogen Production. Energy & Fuels. 33,1296-1301.

Carmignano, O.R., Vieira, S.S., Teixeira, A.P.C., Lameiras, F.S., Brandão, P.R., Lago, R.M., 2021. Iron Ore Tailings: Characterization and Applications. Journal of Brazilian Chemical Society. 32, 10, 1895-1911.

Cho, H. H.; Strezov, V.; Evans, T.J., 2024. Life cycle assessment of renewable hydrogen transport by liquid organic hydrogen carriers. Journal of Cleaner Production. 469, 143130.

Deng, J., Ning, X., Shen, J., Ou, W., Chen, J., Qiu, G., Wang, Y., He, Y., 2022. Biomass waste as a clean reductant for iron recovery of iron tailings by magnetization roasting. Journal of Environmental Management. 317,115435.

Dhyani, V., Bhaskar, T., 2018. A comprehensive review on the pyrolysis of lignocellulosic biomass. Renewable Energy. 129,695-716.

Dudchenko, N., Ponomar, V., Ovsiienko, V., Cherevko, Y., Perelshtein, I., 2024. Mineral Magnetic Modification of Fine Iron Ore Tailings and Their Beneficiation in Alternating Magnetic Fields. Metals. 14:26.

Ghosh, D., Roy, A.K., Ghosh, A., 1986. Reduction of Ferric Oxide Pellets with Methane. Transactions ISIJ. 26 (3), 186 - 193.

Gonçalves, M.V.B.; Mendonça, L.M.; Flores, I.V.; Bagatini, M.C. 2024. Investigation of the Phenomena Associated with Iron Ore Reduction by Raw Biomass and Charcoal Volatiles. Journal of Sustainable Metallurgy.10, 1094 – 1111.

Hata, Y., Purwanto, H., Hosokai, S., Hayashi, J., Kashiwaya, Y., Akiyama, T., 2009. Biotar Ironmaking Using Wooden Biomass and Nanoporous Iron Ore. Energy & Fuels. 23,1128-1131.

Kan, T., Strezov, V., Evans, T.J., 2016. Lignocellulosic biomass pyrolysis: A review of product properties and effects of pyrolysis parameters. Renewable and Sustainable Energy Reviews. 57,1126-1140.

Kim, J., Sovacool, B.K., Bazilian, M., Griffiths, S., Lee, J., Yang, M., Lee, J., 2022. Decarbonizing the iron and steel industry: A systematic review of sociotechnical systems, technological innovations, and policy options. Energy Research & Social Science. 89,102565.

Kumar, M., Upadhyay, S.N., Mishra, P.K., 2022. Pyrolysis of Sugarcane (Saccharum officinarum L.) Leaves and Characterization of Products. ACS Omega. 7,28052-28064.

Kumar, R.; Strezov, V.; Weldekidan, H.; He, J.; Singh, S.; Kan, T.; Dastjerdi, B., 2023. Lignocellulose Biomass Pyrolysis for Bio-Oil Production: Biomass Pre-treatment Methods for Production of Drop-In Fuels, in: Singh, Y.; Strezov, V.; Negi, P., Biowaste and Biomass in Biofuel Applications. CRC Press, Boca Raton, pp.123-196.

Kurniawan, A., Abe, K., Nomura, T., Akiyama, T., 2018. Integrated Pyrolysis–Tar Decomposition over Low-Grade Iron Ore for Ironmaking Applications: Effects of Coal-Biomass Fuel Blending. Energy & Fuels. 32, 1,396-405.

Lanjekar, P. R., Panwar, N.L., Agrawal, C., 2023. A comprehensive review on hydrogen production through thermochemical conversion of biomass for energy security. Bioresource Technology Reports. 21,101293.

Levandoski, W.M.K., Ferrazo, S.T., Bruschi, G.J., Consoli, N.C., Korf, E.P., 2023. Mechanical and microstructural properties of iron mining tailings stabilized with alkali-activated binder produced from agro-industrial wastes. Scientific Reports. 13,15754.

Li, B., Mbeugang, C.F.M., Huang, Y., Liu, D., Wang, Q., Zhang, S., 2022. A review of CaO based catalysts for tar removal during biomass gasification. Energy 244, 123172.

Li, Y., Zhang, Q., Yuan, S., Yin, H., 2021. High-efficiency extraction of iron from early iron tailings via the suspension roasting-magnetic separation. Powder Technology. 379,466-477.

Lin, T-Y., Kuo, C-P., 2012. Study of products yield of bagasse and sawdust via slow pyrolysis and iron-catalyze. Journal of Analytical and Applied Pyrolysis. 96,203-209.

Long, H.; Zhu, D.; Pan, J.; Li, S.; Yang, C.; Guo, Z.; Xu, X., 2024. A critical review on metallurgical recovery of iron from iron ore tailings. Journal of Environmental Chemical Engineering. 12, 2, 112140.

Naono, H., Nakai, K., Sueyoshi, T., Yagi, H., 1987. Porous Texture in Hematite Derived from Goethite: Mechanism of Thermal Decomposition of Goethite. Journal of Colloid and Interface Science, 120,2,439-450.

Ni, M., Leung, D. Y. C., Leung, M. K. H.; Sumathy, K., 2006. An overview of hydrogen production from biomass. Fuel Processing Technology. 87,461-472.

Nordgreen, T., Nemanova, V., Engvall, K., Sjöström, K., 2012. Iron-based materials as tar depletion catalysts in biomass gasification: Dependency on oxygen potential. Fuel. 95,71-78.

Pinto, P. S., Milagre, L.E., Moreira, L.C.M., Junior, H.P.R., Salviano, A.B., Ardisson, J.D., Parreira, F.V., Teixeira, A.P.C., Lago, R.M., 2022. Iron Recovery from Iron Ore Tailings by Direct Hydrogen Reduction at Low Temperature and Magnetic Separation. Journal of Brazilian Chemical Society. 33, 8,969-977.

Ptáček, P., Frajkorová, F., Šoukal, F., Opravil, T., 2014. Kinetics and mechanism of three stages of thermal transformation of kaolinite to metakaolinite. Powder Technology. 264,439-445.

Qiu, G., Ning, X., Shen, J., Wang, Y., Zhang, D., Deng, J., 2023. Recovery of iron from iron tailings by suspension magnetization roasting with biomass-derived pyrolytic gas. Waste Management. 255-263.

Sahu, S.N., Meikap, B.C., Biswal, S.K., 2022. Magnetization roasting of waste in ore beneficiation plant tailings using sawdust biomass; A novel approach to produce metallurgical grade pellets. Journal of Cleaner Production. 343,130894.

Shen, D.K., Gu, S., Bridwater, A.V., 2010. The thermal performance of the polysaccharides extracted from hardwood: Cellulose and hemicellulose. Carbohydrate Polymers. 82,39-45.

Strezov, V., Evans, T.J., Hayman, C., 2008. Thermal conversion of elephant grass (Pennisetum Purpureum Schum) to bio-gas, biooil and charcoal. Bioresource Technology. 99,17,8394–8399.

Sun, Y., Zhu, X., Han, Y., Li, Y., 2019. Green magnetization roasting technology for refractory iron ore using siderite as a reductant. Journal of Cleaner Production. 206, 40-50.

Suopajärvi, H., Kemppainen, A., Haapakangas, J., Fabritius, T., 2017. Extensive review of the opportunities to use biomass-based fuels in iron and steelmaking processes. Journal of Cleaner Production. 148,709-734.

Suopajärvi, H., Umeki, K., Mousa, E., Hedayati, A., Romar, H., Kemppainen, A., Wang, C., Phounglamcheik, A., Tuomikoski, S., Norberg, N., Andefors, A., Öhman, M.; Lassi, U., Fabritius, T.,2018. Use of biomass in integrated steelmaking – Status quo, future needs and comparison to other low-CO_2 steel production technologies. Applied Energy. 213,384-407.

Sutton, D., Kelleher, B., Ross, J.R.H., 2001. Review of literature on catalysts for biomass gasification. Fuel Processing Technology. 73,3,155-173.

Uçar, S., Karagöz, S., 2009. The slow pyrolysis of pomegranate seeds: The effect of temperature on the product yields and bio-oil properties. Journal of Analytical and Applied Pyrolysis. 84,151-156.

Vassilev, S. V., Vassileva, C. G., Vassilev, V.S., 2015. Advantages and disadvantages of composition and properties of biomass in comparison with coal: An overview. Fuel. 158,330-350.

Wang, P., Ryberg, M., Yang, Y., Feng, K., Kara, S., Hauschild, M., Chen, W-Q., 2021. Efficiency stagnation in global steel production urges joint supply- and demand-side mitigation efforts. Nature Communications. 12,2066.

Xu, Y.; Li, E.; Zhang, Y.; Hong, L.; Yao, X., 2024. Research status of new technology for magnetization roasting and reduction of refractory iron ore in China. Minerals Engineering. 218, 109041.

Yang, H., Yan, R., Chen, H., Lee, D.L., Zheng, C., 2007. Characteristics of hemicellulose, cellulose, and lignin pyrolysis. Fuel. 86,1781-1788.

Zhang, X., Han, X., Sun, Y., Lv, Y., Li, Y., Tang, Z., 2019. An Novel Method for Iron Recovery from Iron Ore Tailings with Pre-Concentration Followed by Magnetization Roasting and Magnetic Separation. Mineral Processing and Extractive Metallurgy Review. 41, 2,117-129.

Zhong, R., Yi, L., Huang, Z., Jiang,X., Cai,X., 2020. Reduction Mechanism and Kinetics of a Low Grade Iron Ore-coal Composite Pellets Improved by Sodium Salt. ISIJ International. 60,4,649-655.

Zhu, Y.; Liu, D.; Tan, Z.; Liu, H.; Kan, T.; Zhang, W.; Li, H.; Li, Y.; Yang, W.; Yang, H., 2024. Volatile-char interactions during co-pyrolysis of sewage sludge and poplar wood. Journal of the Energy Institute. 117, 101820.

Zulkania, A., Rochmadi, R., Cahyono, R.B., Hidayat, M., 2021. Investigation into Biomass Tar-Based Carbon Deposits as Reduction Agents on Iron Ore Using the Tar Impregnation Method. Metals, 11,10:1623.

4. CONSIDERAÇÕES FINAIS

No presente trabalho foram avaliadas as interações entre os voláteis liberados durante a pirólise de diferentes biomassas com o minério de ferro e com o rejeito de mineração de ferro. O objetivo foi compreender a fenomenologia e os mecanismos envolvidos no processo simultâneo de pirólise e redução de óxidos de ferro, visando avaliar a viabilidade do uso dos voláteis de biomassa para aprimorar as características magnéticas das fases de ferro contidas nos rejeitos ultrafinos de mineração de ferro, promover a deposição de carbono nas partículas ferrosas e aumentar sinergicamente a produção de hidrogênio biogênico.

O estudo apresentado no Capítulo 2 investigou os fenômenos associados ao uso dos produtos voláteis derivados do eucalipto *in natura* e do carvão vegetal como agentes redutores de minério de ferro granulado. Primeiramente, a análise dos gases revelou que as pirólises das duas biomassas produziram principalmente CH_4, CO, CO_2 e H_2. Ressalta-se que durante a pirólise do eucalipto *in natura*, o gás majoritário foi o CO, enquanto o carvão vegetal gerou principalmente o H_2. Ao se realizar a pirólise do eucalipto *in natura* na presença do minério de ferro, observou-se uma diminuição no rendimento de CO e H_2, enquanto o CO_2 aumentou. Já com o carvão vegetal, houve um aumento no rendimento de CO e CO_2, com uma diminuição no H_2. A análise mineralógica mostrou que os voláteis de ambas as biomassas promoveram a redução dos óxidos de ferro do minério, sendo que as condições que favoreceram o progresso das reações de redução incluíram o uso dos voláteis do carvão vegetal e minério de tamanhos médio e fino. Além disso, os ensaios interrompidos a 600 ºC mostraram a capacidade dos voláteis das biomassas em depositar carbono na superfície do minério de ferro, a partir do craqueamento catalítico do alcatrão, sendo mais relevante ao se usar eucalipto *in natura*. A morfologia da wüstita formada a partir do carvão vegetal foi mais densa e compacta, indicando que o hidrogênio foi o principal agente redutor. Por outro lado, a superfície da wüstita formada pela redução com os voláteis do eucalipto *in natura* foi menos compacta e mais porosa, sugerindo que o carbono depositado foi o agente redutor predominante. Os resultados indicaram que a pirólise de ambas as biomassas produz compostos voláteis que podem desempenhar um papel crucial na produção do ferro e aço. Além de serem materiais renováveis, que podem contribuir com uma redução significativa nas emissões líquidas de CO_2 a partir do processo siderúrgico, esses produtos podem contribuir com a eficiência energética, fornecendo agentes redutores adicionais; com a flexibilidade operacional e com possíveis benefícios econômicos. A redução no consumo de energia e os menores custos de conformidade ambiental devido à

redução das emissões podem contribuir para economias de custo. Além disso, o melhor aproveitamento dos produtos da biomassa pode contribuir com a redução da dependência de combustíveis fósseis importados.

A partir de uma análise detalhada dos gases e dos fenômenos que governam as interações da matéria volátil da biomassa com óxidos de ferro apresentada no Capítulo 2, o Capítulo 3 focou na avaliação de diferentes condições que favoreçam a transformação mineralógica de óxidos de ferro e a sua recuperação magnética, a deposição de carbono nas partículas ferrosas e a geração de hidrogênio biogênico, a partir a pirólise de bagaço de cana-de-açúcar (SCB) na presença de micropelotas de rejeito de mineração de ferro (IOT). Além da temperatura, os experimentos demonstraram que a razão mássica entre SCB e IOT é um parâmetro que exerce influência na transformação mineralógica do material ferroso e na sua recuperação magnética, na quantidade de carbono depositado e na produção de gases. Os maiores rendimentos de gás por grama de biomassa foram alcançados com a menor razão SCB/IOT em todas as temperaturas avaliadas. Transformações mineralógicas mais avançadas foram observadas quando o processo de pirólise e redução aconteceu a 1000 °C, resultando em wüstita, faialita e ferro metálico. A proporção de biomassa influenciou a formação de ferro metálico, onde o teste com maior relação mássica SCB/IOT favoreceu a metalização do IOT. Entretanto, os processos de pirólise e pré-redução a 400, 600 e 800 °C resultaram em diferentes fases predominantes: hematita, magnetita e uma mistura de magnetita e wüstita, respectivamente. Nesta mesma relação mássica, a recuperação magnética e a deposição de carbono nas micropelotas de rejeito de mineração foram maximizadas a 600 °C. No entanto, a menor relação mássica entre SCB e IOT foi benéfica para aumentar a produção de H_2. Este resultado sugere que o contato íntimo entre o catalisador e o alcatrão foi fundamental para a eficácia catalítica e, portanto, para aumentar a produção de hidrogênio. Esta Tese indicou que a temperatura ideal para promover a recuperação de ferro a partir da técnica de magnetização dos rejeitos de minério de ferro foi 600 °C, onde em todos os testes nesta temperatura foi possível obter uma recuperação magnética superior a 90%, evitando a formação de fases que dificultem essa separação. Os experimentos demonstraram que o uso de uma maior relação mássica SCB/IOT foi essencial para que a recuperação atingisse até 98%. Esses resultados propõem uma abordagem tecnicamente viável para valorizar sinergicamente rejeitos de minério de ferro e bagaço de cana-de-açúcar. Entretanto, uma análise de disponibilidade do bagaço de cana associada a demanda desse material em outros processos, como a produção de etanol de segunda geração (Etanol-2G) e a cogeração de energia elétrica, precisa ser cuidadosamente realizada (Carpio & Souza, 2019). Por fim, a recuperação da fração

magnética contendo carbono depositado oferece um método alternativo para a produção de aglomerados autorredutores para a indústria siderúrgica.

Neste trabalho foi possível demonstrar que a utilização de voláteis de biomassa para pré-redução de minério de ferro granulado e recuperação de ferro de rejeitos de mineração é uma alternativa para contribuir com o melhor aproveitamento dos voláteis da biomassa com consequente redução do consumo de combustíveis fósseis na indústria siderúrgica e mitigar os impactos negativos associados ao armazenamento de rejeitos em barragens. A integração de processos de produção de carvão vegetal/biocarbono com estações de pré-redução de óxidos de ferro pode configurar uma alternativa para aproveitar de forma eficiente os produtos líquidos e gasosos resultantes do processo de conversão termoquímica da biomassa, além de enriquecer os gases de pirólise em hidrogênio biogênico. Particularmente os produtos condensáveis, frequentemente considerados problemáticos nas instalações industriais, podem ser reaproveitados sem a necessidade de estações de condensação complexas e de alto custo. O uso desses voláteis para purificar rejeitos de mineração de ferro pode se tornar uma alternativa economicamente viável, mitigando as perdas de ferro no beneficiamento de minérios de baixo teor e aumentando a disponibilidade de matérias-primas para os processos de produção de ferro.

4.1. Referências

Carpio, L. G. T., Souza, F.S., 2019. Competition between Second-Generation Ethanol and Bioelectricity using the Residual Biomass of Sugarcane: Effects of Uncertainty on the Production Mix. Molecules. 24,2, 369.

5. CONTRIBUIÇÕES ORIGINAIS AO CONHECIMENTO

As principais contribuições deste trabalho para o avanço do conhecimento científico e do desenvolvimento tecnológico a respeito das interações da matéria volátil de biomassas com partículas ricas em óxidos de ferro foram:

1. A compreensão das interações entre os voláteis da biomassa e o minério de ferro, oferece uma alternativa para a utilização de matéria-prima renovável nos processos de produção de ferro. As vazões individuais dos gases liberados durante o processo de pirólise foram avaliadas quantitativamente, tanto para o eucalipto *in natura* quanto para o eucalipto carbonizado. O efeito catalítico dos óxidos de ferro sobre a matéria volátil condensável e seu impacto no perfil de liberação dos gases também foram detalhadamente analisados. A contribuição de cada agente redutor para o avanço das reações de redução dos óxidos de ferro, assim como a influência na evolução microestrutural dos produtos, enriquece a literatura disponível, proporcionando uma compreensão aprofundada da fenomenologia envolvida na interação entre os óxidos de ferro e a matéria volátil liberada da biomassa *in natura* e do carvão vegetal. Este conhecimento oferece subsídios para o aproveitamento da matéria volátil condensável e não condensável, geradas nos processos de produção de biocarbono, nos processos de redução de óxidos de ferro;

2. A Tese apresentou uma abordagem detalhada para a valorização sinérgica do bagaço de cana-de-açúcar e da fração ultrafina dos rejeitos de mineração de ferro, promovendo a economia circular e a utilização de resíduos industriais. A pesquisa demonstrou condições favoráveis de temperatura e proporção de biomassa/rejeitos de mineração de ferro para maximizar a recuperação de ferro e a deposição de carbono, além de aumentar a produção de hidrogênio. Esses resultados oferecem uma alternativa tecnicamente viável para purificar rejeitos de mineração de ferro por meio do uso dos voláteis liberados durante a pirólise do bagaço de cana-de-açúcar, além de ser uma rota alternativa para a produção de hidrogênio biogênico. A transformação desses materiais em coprodutos contribui com a mitigação dos impactos associados a estocagem desse rejeito e resulta na produção de matérias-primas alternativas para a indústria siderúrgica tradicional, bem como a possibilidade de produção de aglomerados autorredutores com menor exigência de adição de carbono.

6. CONTRIBUIÇÕES PARA A LITERATURA

6.1. Publicações geradas a partir da presente tese

6.1.1. Artigos publicados em periódicos

Gonçalves, M.V.B.; Mendonça, L.M.; Flores, I.V.; Bagatini, M.C. 2024. **Investigation of the Phenomena Associated with Iron Ore Reduction by Raw Biomass and Charcoal Volatiles**. Journal of Sustainable Metallurgy. 10, 1094-1111. https://doi.org/10.1007/s40831-024-00851-0, Qualis A2.

Gonçalves, M.V.B.; Rocha, J.V.M.; Flores, I.V.; Bagatini, M.C. **Sugarcane bagasse and iron ore tailings thermochemical conversion towards sustainable iron recovery with biogenic carbon and hydrogen production**. Journal of Cleaner Production. 482, 144219. https://doi.org/10.1016/j.jclepro.2024.144219, Qualis A1.

6.1.2. Artigos publicados em anais de congresso

Gonçalves, M.V.B.; Bagatini, M.C.; Mendonça, L.M. **Investigação dos fenômenos envolvidos na redução do minério de ferro por voláteis de biomassa *in natura* e carvão vegetal**. In: 51º Seminário de Redução de Minérios e Matérias-Primas, São Paulo, 2023. 51º Seminário de Redução de Minérios e Matérias-primas, 2023. v. 51, p. 676-687.

Mendonça, L.M.; Gonçalves, M.V.B.; Bagatini, M.C. **Uso dos gases de pirólise de biomassa na redução de minério de ferro**. In: 21º Encontro Nacional de Estudantes de Engenharia Metalúrgica, de Materiais e de Minas (ENEMET), São Paulo, 2023. 21º Encontro Nacional de Estudantes de Engenharia Metalúrgica, de Materiais e de Minas (ENEMET), 2023. v.21, p. 214-221.

Gonçalves, M.V.B.; Rocha, J.V.M.; Flores, I.V.; Bagatini, M.C. **Conversão Sinérgica de Bagaço de Cana e Rejeitos de Mineração de Ferro**. In: 52º Seminário de Redução de Minérios e Matérias-Primas, São Paulo, 2024. 52º Seminário de Redução de Minérios e Matérias-Primas, 2024. v.52, p.581-595.

Rocha, J.V.M.; Gonçalves, M.V.B.; Bagatini, M.C. **Recuperação de Ferro a Partir de Rejeitos de Mineração de Ferro e Voláteis de Biomassa**. In: 22º Encontro Nacional de Estudantes de Engenharia Metalúrgica, de Materiais e de Minas (ENEMET), São Paulo, 2024. 22º Encontro Nacional de Estudantes de Engenharia Metalúrgica, de Materiais e de Minas (ENEMET), 2024. v.22, p.724-735.

6.2. Outas publicações no decorrer da formação acadêmica

6.2.1. Publicações em periódicos

Lau, L.L.; Strezov, V.; Gonçalves, M.V.B.; Bagatini, M.C. **Trace elements emission in iron ore sintering: A review**. 2021. Environmental Advances. v.6. 100123. https://doi.org/10.1016/j.envadv.2021.100123

6.2.2. Publicações em anais de congressos

Gonçalves, M.V.B.; Campos, A.; Agra, A.; Figueiró, C.; Benevides, J.; Gonçalves, G.; Oliveira, R.; Potter, S. **Pré-redução de briquetes utilizando gás de topo do Tecnored Recycler**. In: 51º Seminário de Redução de Minérios e Matérias-Primas, São Paulo, 2023. 51º Seminário de Redução de Minérios e Matérias-primas, 2023. v. 51. p. 637-649.

Campos, A.M.A.; Amorim, M.R.; Gonçalves, M.V.B.; Agra, A.A.; Figueiró, C.G.; Marcondes, E.V.; Gonçalves, G.F.; Oliveira, R.; Potter, S.M. **Tecnored BBC (Bio-briquette for cokemaking): avaliação laboratorial do uso de briquetes na coqueria**. In: 51º Seminário de Redução de Minérios e Matérias-Primas, São Paulo, 2023. 51º Seminário de Redução de Minérios e Matérias-primas, 2023. v. 51. p. 396-409.

Agra, A.A.; Campos, A.; Rocha, M.; Gonçalves, M.; Benevides, J.; Gonçalves, G.; Oliveria, R.; Potter, S. **Tecnored - Catalyzed Briquettes for Blast-furnace**. In: 51º Seminário de Redução de Minérios e Matérias-Primas, São Paulo, 2023. 51º Seminário de Redução de Minérios e Matérias-primas, 2023. v. 51. p.650-661.

Figueiró, C.G.; Gonçalves, M.V.B.; Campos, A.; Agra, A.; Gonçalves, C.S.; Gonçalves, G.; Oliveira, R.; Potter, S. **Tecnologia de carbonização Tecnored: Produção sustentável de biocarbono para descarbonização da indústria siderúrgica**. In: 51º Seminário de Redução de Minérios e Matérias-Primas, São Paulo, 2023. 51º Seminário de Redução de Minérios e Matérias-primas, 2023. v. 51. p.462-475.

Gonçalves, M.V.B.; Agra, A.; Figueiró, C.; Fialho, L.; Benevides, J.; Gonçalves, G.; Luz, A.; Oliveira, R.; Potter, S. **Recuperação de zinco a partir do forno Tecnored Recycler – uma nova rota pirometalúrgica para concentração de zinco**. In: 52º Seminário de Redução de Minérios e Matérias-Primas, São Paulo, 2024. 52º Seminário de Redução de Minérios e Matérias-Primas, 2024. v.52, p.398-409.

Figueiró, C.G.; Gonçalves, M.V.B.; Agra, A.; Fialho, L.F.; Braga, J.R.; Gonçalves, G.; Oliveira, R.; Potter, S. **Potencial das simulações DEM e CFD na otimização de tecnologias industriais: um estudo de caso de reatores rotativos de secagem e pirólise**. In: 52º Seminário de Redução de Minérios e Matérias-Primas, São Paulo, 2024. 52º Seminário de Redução de Minérios e Matérias-Primas, 2024. v. 52, p.518-528.

Fialho, L.F.; Rocha, M.A.; Agra, A.; Figueiró, C.G.; Gonçalves, M.V.B.; Oliveria, M.; Benevides, J.P.; Gonçalves, G.; Oliveria, R.; Potter, S. **Desenvolvimento de briquete termo redutor (BTR) para utilização em altos-fornos a carvão vegetal**. In: 52º Seminário de Redução de Minérios e Matérias-Primas, São Paulo, 2024. 52º Seminário de Redução de Minérios e Matérias-Primas, 2024. v.52, p.529-537.

7. SUGESTÕES PARA TRABALHOS FUTUROS

Os seguintes temas são sugeridos como trabalhos futuros:

1. Avaliar a qualidade dos *chars* produzidos a partir da pirólise do eucalipto *in natura*, do eucalipto carbonizado e do bagaço de cana-de-açúcar e inferir os possíveis usos desses materiais como fontes de energia. Sugere-se avaliar o desempenho da mistura desses biomateriais durante e após processos de aglomeração à frio e à quente, *i.e*., briquetagem, pelotização e sinterização;

2. Avaliar experimentalmente o impacto das diferentes morfologias do minério de ferro pré-reduzido, formadas com os voláteis do eucalipto *in natura* e do carvão vegetal, na progressão das reações de redução;

3. Caracterizar química, mineralógica e morfologicamente as frações magnética e não-magnética do rejeito de mineração de ferro. Avaliar a susceptibilidade magnética das fases e verificar a possibilidade de separação magnética de baixa intensidade;

4. Investigar diferentes proporções de adição de minério e rejeito de mineração de ferro, pré-reduzido e impregnado com carbono, em misturas autorredutoras, aglomerar, realizar testes de autorredução e comparar com o desempenho de materiais convencionais;

5. Avaliar de forma teórica e a prática a integração de rejeitos de mineração de ferro e de minério de ferro ultrafino em estações contínuas, pilotos e industriais, de conversão termoquímica de biomassa. Estes testes podem escalonar o uso de materiais ferrosos como filtros dos materiais condensáveis, contribuindo com o aumento da produtividade e redução de incrustações em tubulações, além de serem preparados para etapas subsequentes dentro da rota siderúrgica;

6. Avaliar a purificação das misturas gasosas obtidas a partir da pirólise e da conversão sinérgica das biomassas e dos óxidos de ferro a partir de métodos disponíveis na literatura;

7. Realizar análises de ciclo de vida para avaliar o impacto ambiental total do processo, incluindo emissões de gases de efeito estufa, consumo de energia e recursos, disponibilidade de matérias-primas e benefícios ambientais em comparação com processos tradicionais de redução de óxidos de ferro e disposição de rejeitos de mineração de ferro.